Device-Free Localization: A Review of Non-RF Techniques for Unobtrusive Indoor Positioning

Fakhrul Alam, *Senior Member, IEEE*, Nathaniel Faulkner, and Baden Parr

***Abstract*—Accurate, reliable indoor localization or positioning is the key enabler for location-based services. Indoor localization can be broadly classified into two distinct categories. Active localization entails tracking a tag attached to or carried by the target. Passive localization, on the other hand, involves positioning a device-free or untagged target. While passive or device-free localization is comparatively more difficult to achieve, it is the preferred option for many applications. Vision-based techniques can accurately localize an untagged target. However, privacy is a significant concern and thus have limited usability for many applications, especially in noncommercial and residential settings. Passive localization using radio frequency (RF) or wireless sensing is an unobtrusive option and has seen extensive research efforts in recent years leading to a saturated research field but no consensus solution. Researchers have been investigating alternative solutions that can facilitate robust passive localization. The rapid proliferation of Internet of Things (IoT) is bringing ubiquitous networked devices and ambient sensors into modern buildings. The consequential pervasive ambient intelligence and signals of opportunity can enable unobtrusive device-free positioning. This article presents a comprehensive review of non-RF solutions covering visible light-, infrared-, physical excitation- and electric field sensing-based techniques. Limitations of the state-of-the-art and potential future research directions are also outlined.**

***Index Terms*—Ambient assisted living (AAL), capacitive sensing, cyber–physical systems, device-free localization (DFL), electric field sensing, human–computer interaction (HCI), human sensing, indoor localization, indoor positioning system (IPS), infrared (IR) sensing, Internet of Things (IoT), passive IR (PIR), passive positioning, smart building, smart home, vibration-based localization, visible light positioning (VLP).**

I. Introduction

INDOOR localization has been an active research topic for more than two decades. While outdoor positioning (e.g., GPS) is a mature technology, it does not work reliably inside buildings and there is no standardized solution for indoor positioning system (IPS) yet. Location-based services (LBSs) within the built environment require robust and affordable positioning. The rapid adoption of Internet of Things (IoT) [1] is providing access to a ubiquitous network of devices and ambient sensors. This is opening up new opportunities for deploying IPS leveraging preexisting infrastructure.

Indoor localization can be broadly categorized into active and passive localization. Active localization is similar to GPS-based positioning where the target carries a device (or a tag). The positioning of the tag results in localizing the target. Active localization is useful for applications, such as asset tracking, navigation of mobile robots, and many other use cases, where the end user is carrying a device (e.g., a mobile phone). A multitude of options, e.g., computer vision [2], light detection and ranging (LIDAR) [3], ultrasound [4], acoustic [5], geomagnetic fingerprinting [6], wireless or radio frequency (RF) [7], visible light [8], aroma fingerprinting [9], etc., have been investigated for active indoor localization. However, for many applications, relying on the target to carry a tag is not feasible. If the goal is to unobtrusively track an elderly, forgetful person, one cannot expect them to wear a tag (e.g., a bracelet) every day. The wearable device can also be forgotten or misplaced, get damaged or may require frequent battery changes. Having to carry a "tracking" device can be perceived as stigmatizing leading to reluctance to wear one. Passive localization, also known as device-free localization (DFL), is the method of localizing an untagged target. It does not require the target to actively participate in the localization process by carrying a tag.

Passive localization is the key to providing ambient-assisted living (AAL) in smart buildings. The application of DFL ranges from intrusion detection, fall detection and remote monitoring of the elderly, occupancy detection for energy-efficient heating, ventilation, and air conditioning (HVAC) and lighting, occupancy counting for emergency situations, such as the evacuation of offices and public buildings, business analytics for retail applications, accessibility aids for visually impaired individuals, etc.

Based on the sensing modality, passive localization can be divided into six major categories: 1) vision-; 2) RF-; 3) visible light-; 4) infrared-; 5) physical excitation-; and 6) electric field sensing-based techniques. The physical excitation methods can be further classified into localization using pressure and vibration sensing. The electric field sensing techniques, sometimes termed capacitive sensing, include both active and passive sensing. The DFL classification is shown in Fig. 1. It should be noted that environmental sensors (e.g., temperature, relative humidity etc.) can accurately infer occupancy [10], but by themselves are not suitable for fine-grained application such as localization. Similarly, CO_2 sensors are commonly used for occupancy detection [11]. However, their slow response time,

Manuscript received July 21, 2020; revised September 23, 2020; accepted October 8, 2020. Date of publication October 13, 2020; date of current version March 5, 2021. The work of Nathaniel Faulkner was supported in part by the Massey University Doctoral Scholarship. *(Corresponding author: Fakhrul Alam.)*

The authors are with the Department of Mechanical and Electrical Engineering, School of Food and Advanced Technology, Massey University, Auckland 0632, New Zealand (e-mail: f.alam@massey.ac.nz; n.faulkner@massey.ac.nz; b.parr@massey.ac.nz).

Digital Object Identifier 10.1109/JIOT.2020.3030174

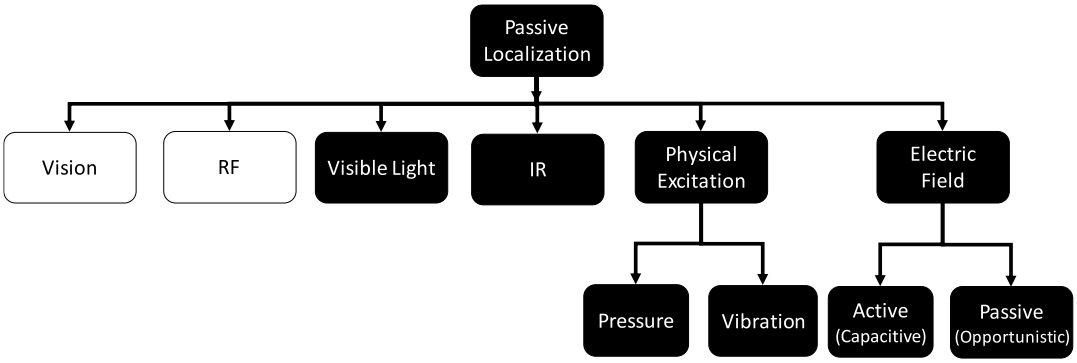

Fig. 1. Classification of DFL based on sensing modality. Vision- and RF-based techniques are not covered by this article.

TABLE I
RECENT SURVEY ARTICLES ON INDOOR LOCALIZATION

RESEARCH	SENSING TECHNIQUE	DFL?	COVERS NON-RF?
Teixeira et al. [35] [a] ,2010	**Multiple**	✓	✓
Yang et al. [25], 2015	RF	×	×
He at al. [27], 2015	RF	×	×
Xiao et al. [29], 2016	RF	✓	×
Yassin et al. [7], 2016	RF	×	×
Luo et al. [30], 2017	Visible Light	×	✓
Brena et al. [36], 2017	**Multiple**	×	✓
Grosse-Puppendahl et al. [34], 2017	Electric Field	✓	✓
Jang et al. [26], 2018	RF	×	×
Lashkari et al. [28], 2018	RF	×	×
Zhuang et al. [31], 2018	Visible Light	×	✓
Keskin et al. [32], 2018	Visible Light	×	✓
Ma et al. [18], 2019	RF	✓	×
Shit et al. [21], 2019	RF	✓	×
Zafari et al. [22], 2019	RF	✓	×
Denis et al. [23], 2019	RF	✓	×
Al-qaness et al. [24], 2019	RF	✓	×
Afzalan et al. [33], 2019	Visible Light	×	✓
Khelifi et al. [37] [b], 2019	**Multiple**	✓	✓
Maheepala et al. [8], 2020	Visible Light	×	×
Alam et al. (This article)	**Multiple**	✓	✓

[a] Dated article
[b] Discusses both active and passive localization; majority of the non-obtrusive sensing techniques for DFL not covered

sensitivity to environment, dependence on external factors (e.g., ventilation), and sparse deployment [12] make them unsuitable for localization.

Camera- or vision-based techniques are widely used for surveillance [13], crowd counting [14], etc. Several studies have indicated that low-cost 3-D cameras (e.g., Kinect) may be suitable for DFL purposes [15], [16]. However, vision-based techniques require favorable lighting conditions and have coverage blind spots due to occlusion. Most importantly, privacy concerns [17] make camera-based IPS in residential environments impractical. This is somewhat ironic given the ubiquitous presence of cameras embedded in smartphones, computing devices, gaming consoles, etc., in modern households. We have therefore excluded vision-based localization techniques from this survey.

Localization based on RF sensing can potentially utilize the preexisting wireless network of a building. It can also operate in "through walls" scenarios. DFL solutions employing customized hardware and the channel state information (CSI) metric can be quite accurate with median error reaching below half a meter [18], [19]. However, CSI is only available with Wi-Fi and thus preclude the majority of wireless technologies (e.g., Bluetooth, ZigBee, etc.). Utilization of the universally available received signal strength indicator (RSSI) lowers the accuracy and requires a significant number of wireless nodes to function [20]. This takes away the appeal of localization with preexisting infrastructure. The survey of the wireless DFL literature shows a vast discipline with a crowded research landscape leading to a high entry barrier for researchers. RF-based passive positioning is also well catered for with many recent review articles. Interested readers are directed toward the survey papers and the articles within [18], [21]–[24]. RF or wireless DFL techniques have, therefore, been excluded from our article.

A. Contribution

There are many good review articles on indoor localization, published in reputable journals, as listed in Table I. However, the existing surveys either do not cover DFL or focus only on RF-based DFL or have been overtaken by significant technological and conceptual advances. For example, review articles [18] and [21]–[24] consider only RF sensing-based passive positioning. Articles [7] and [25]–[28] consider various aspects of RF-based active localization techniques, predominantly focusing on localizing a target carrying a smartphone. Both active and passive positioning based on only RF sensing are discussed in [29] whereas only active visible light positioning (VLP) is considered in [8] and [30]–[33]. Passive positioning using electric field or capacitive sensing is addressed in [34]. However, this article only considers electric field sensing, and localization is merely one among a multitude of human computer interaction (HCI) applications covered. A comprehensive survey that covers passive positioning using a large variety of sensing techniques can be found in the 2010 article [35]. Given the fast-moving pace of localization research and the progress achieved in the last decade, this excellent article has unfortunately become dated. For example, the concept of VLP for passive localization was reported more than five years after this article was published. A 2017 survey covering several sensing techniques can be found in [36]. Nevertheless, this article only considers device-based or active localization. Another survey covering DFL was reported in 2019 [37]. However, this article discusses both active and passive positioning, does not consider indoor localization only and also does not cover many of the unobtrusive techniques available for DFL. Therefore, there is a clear need for a comprehensive review on passive indoor localization techniques that do not use RF sensing. Our article offers the following contributions.

1) An extensive overview of unobtrusive passive positioning facilitated by non-RF sensing techniques, addressing an identified gap in the literature.
2) An in-depth and comprehensive discussion on the limitations of the state of the art leading to opportunities for future research.

Our review discusses works that report positioning (current location of the target) and/or tracking (successive locations of the target). Articles exploring synergistic applications, such as presence or occupancy detection, counting, pose identification, fall detection, target identification, gesture recognition, etc., are not covered unless positioning and/or tracking were also explicitly investigated. We also do not describe basic concepts, such as ranging (estimating the distance of the target from the sensor), positioning methods (e.g., lateration, angulation, etc.), tracking algorithms (e.g., sequence estimators, Kalman, or particle filters), classifiers, etc. Many excellent tutorials and textbooks already cover these topics quite thoroughly.

The following keywords (by themselves and in combinations) were used to search for relevant articles: indoor localization, IPS, DFL, passive positioning, VLP, IR (or infrared) positioning/sensing, capacitive sensing, electric field sensing, Passive IR (PIR), thermopile sensing, vibration-based localization/positioning, human sensing, AAL, location-based service, LBS, etc. Based on our familiarity with the discipline, we decided to start the search in the IEEE XPLORE and ACM digital library databases. Web of Science and Scopus databases were extensively used. Google Scholar (and its "cited by" feature) were also heavily utilized. Given the linkage of localization to biomedical applications, PubMed was also utilized for article search. Publisher websites, e.g., Elsevier (ScienceDirect), Springer, and Hindawi, were also searched for articles along with the social networking site ResearchGate.

The remainder of this article is organized as follows. Section II gives a general overview of visible light-based passive positioning techniques. Section III introduces DFL using

TABLE II
LIST OF ACRONYMS

Acronym	Meaning
AAL	Ambient Assisted Living
ADL	Activities of Daily Living
ANN	Artificial Neural Network
AoA	Angle of Arrival
CNN	Convolutional Neural Network
CSI	Channel State Information
DFL	Device Free Localization
DNN	Deep Neural Network
DoF	Degrees of Freedom
EPS	Electric Potential Sensor
FoV	Field of View
FSR	Force Sensing Resistor
GRF	Ground Reaction Force
GT	Ground Truth
HCI	Human Computer Interaction
HMM	Hidden Markov Model
IoT	Internet of Things
IPS	Indoor Positioning System
IR	InfraRed
KNN	K Nearest Neighbor
LBS	Location Based Service
LED	Light Emitting Diode
LSTM	Long-Short Term Memory
MIMO	Multiple Input Multiple Output
MISO	Multiple Input Single Output
ML	Machine Learning
MLE	Maximum Likelihood Estimator
MLSE	Maximum Likelihood Sequence Estimator
MSE	Mean Square Error
PDA	Probabilistic Data Association
PIR	Passive Infrared
POF	Plastic Optical Fiber
RMSE	Root Mean Squared Error
RSS	Received Signal Strength
RSSI	Received Signal Strength Indicator
SNR	Signal to Noise Ratio
SVM	Support Vector Machine
SVR	Support Vector Regression
TDM	Time Division Multiplexing
TDoA	Time Difference of Arrival
ToA	Time of Arrival
ToF	Time of Flight
VLC	Visible Light Communication
VLP	Visible Light Positioning
WKNN	Weighted K Nearest Neighbor
WSN	Wireless Sensor Network

infrared (IR) sensing. Section IV discusses physical excitation-based passive localization techniques. Section V presents DFL based on electric field sensing. Section VI concludes this article with discussion on shortcomings of state of the art, open research questions, and opportunities for future work. Table II lists all acronyms.

II. DFL With Visible Light Sensing

VLP [38] has attracted considerable interest from the research community in recent years for active localization. VLP systems have the potential to leverage the existing lighting infrastructure and have been gaining popularity in part due to the rapid uptake of energy efficient light emitting diode (LED) technology for illumination. Researchers are also attracted by the synergy that VLP has with the upcoming visible light communication (VLC) [39] and the ready access to light sensors on ubiquitous smartphones. VLP also has some inherent advantages, such as security (signal confined within a relatively small locale), immunity from RF interference, absence of small-scale fading (the wavelength of visible light is much smaller compared to the surface area of a typical light-sensor), etc.

The success of visible light-based active localization has encouraged researchers to explore VLP for device-free positioning. Passive VLP is a relatively new development with the earliest works reported in the literature in 2015 [40]. Some of the reported works demonstrate the potential of passive VLP with the aid of theoretical development and numerical simulations [41], [42]. However, prototype implementations with experimental results and localization performance [43], [44] are becoming more common. Passive VLP systems operate on the premise that the presence of the target alters the optical channel between light sources and light sensors (e.g., photodiodes). These changes are often measured as variations to the light level or illuminance at a light sensor present in the vicinity of the target (see Fig. 2 for an example). The positioning can be inferred from the changes measured at a number of preinstalled sensors at judiciously selected locations (e.g., on the wall [43], [45], ceiling [46], floor [40], etc.).

A. Floor Inlaid With Light Sensors

In this scenario, positioning is determined from the shadows cast by the target onto the floor. Li *et al.* [44] developed StarLight based on this concept. It uses bespoke VLC-enabled luminaires that are modulated for multiplexing purposes. A link between the light-sensor and a luminaire is considered to be shadowed based on a predefined threshold. The prototype uses 20 light sensors along with 20 ceiling mounted LED luminaires within a 3.6 m × 4.8 m area. A mean angular accuracy of 13.6° while detecting the position of a human's body and four major limbs is achieved. It is able to track a mobile skeleton with mean and 95 percentile localization error of 0.04 and 0.097 m, respectively. StarLight is an extension of LiSense [40] that used five luminaires and 324 light sensors within a 3 m × 3 m testbed. While it was not evaluated for localization performance, the prototype was shown to attain a mean angular accuracy of 10° for skeleton reconstruction.

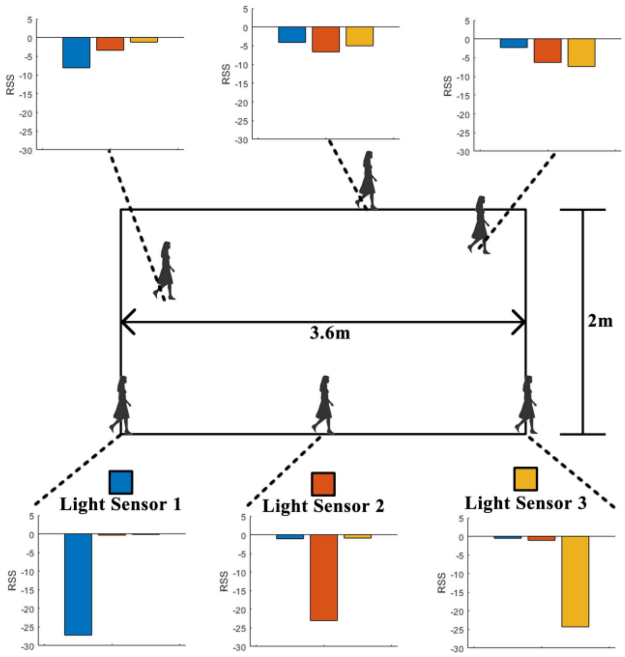

Fig. 2. Drop in ambient light level at three ISL29035 light-sensors for six different positions of a subject (one of the authors) within a 3.6 m × 2 m space. The sensors are mounted on a wall 0.2 m from the boundary of the test.

LocaLight [47] is a prototype system that employs floor-embedded light sensors wirelessly powered by an RFID reader. In contrast to StarLight, standard luminaires are used. The shadows cast by a subject walking between the sensor and the luminaire are detected by the light sensors. With a 1-D testbed of three luminaires and five sensor tags, Di Lascio *et al.* are able to locate a target within a range of 0.5 m.

Zhang *et al.* [41] also proposed to use a grid of light sensors embedded into the floor. LED luminaires, mounted on the ceiling, cast shadows of the target onto the sensors. A luminaire to sensor link is considered to be obstructed if the received signal strength (RSS) dips below a predefined threshold. The positioning is estimated using a geometric model that finds the intersection of the obstructed links. A luminaire to light-sensor link is implemented to measure parameters that are used for numerical simulation. The simulation study reports a median error of 0.08 m in an 8 m × 8 m × 4 m room with four LED luminaires, and 81 light sensors that were inlaid in a 0.5 m × 0.5 m grid on the floor. The system can track multiple targets (up to 10) in theory and simulation using an adaptive multitarget positioning algorithm.

B. Ceiling Mounted Light Sensors

These systems co-locate the light sensors with the luminaires for monitoring (typically the RSS of) the reflected signal at the sensors. The reflected light and therefore, the positioning performance depends on several factors, such as clothing color, walking direction, and luminaire-sensor separation [48].

Eyelight [46] is a VLP system that can track human movement and detect room occupancy based on ceiling mounted sensors. Nguyen *et al.* used time-division multiplexing (TDM) to create orthogonal links between

bespoke LED luminaries and light sensors. For a prototype implementation, they co-locate four light sensors with narrow Field of View (FoV) alongside a luminaire to create a transceiver node. In a 45 m^2 room, Eyelight is able to achieve 0.89 m median positioning error using six ceiling mounted transceiver nodes. A two-stage localization algorithm based on predetermined threshold of RSS at the sensors is employed. The first stage performs coarse detection by identifying movement within the "coverage" of a node. The second stage achieves fine-grained localization by identifying which link is broken. They also report 93.7% occupancy count accuracy and 93.78% activity classification accuracy using Adaboost, a common machine learning (ML) technique. Eyelight is the extension of an earlier work that was able to detect whether a door was open or closed through passive sensing [49].

Majeed and Hranilovic report the theoretical development of a passive VLP system [42] that utilizes the channel sounding approach. This an extension of their earlier work reported in [50]. Light sensors located on the ceiling alongside VLC-enabled luminaires are proposed. A maximum-likelihood estimator (MLE) achieved positioning using the changes caused by the target to the optical channel impulse response between the luminaires (transmitters) and the light sensors (receivers). They suggest using Time-of-Arrival (ToA) and/or Time Difference-of-Arrival (TDoA) methods to measure the channel impulse response. Their simulation results show a root mean-square error (RMSE) of less than 0.1 m. They also derive the Cramer–Rao lower bound of the localization method.

Al-Hameed *et al.* [51] suggested localization by adopting the concept of radar-like reflection of VLC. They undertake the theoretical development of light detection and localization (LiDAL). They propose a multiple-input–multiple-output (MIMO) system with a wide FoV single photodiode-based receiver and a multiple-input–single-output (MISO) system using an imaging receiver. Simulation results show that in an otherwise empty 8 m $\times$ 4 m $\times$ 3 m room with seven targets, the localization RMSE is 0.28 m and 0.16 m for eight ceiling mounted MIMO and MISO systems, respectively. The localization accuracy degrades once furniture is introduced in the simulation environment and the performance degrades further if the target moves in a nomadic, random pattern. A subsequent simulation study [52], shows that an artificial neural network (ANN) can learn the LiDAL induced reflection to improve detection and localization accuracy.

Yang *et al.* [53] employed reverse-biased LED luminaires as photodiodes (i.e., light sensors) for occupancy sensing. While their CeilingSee system that utilized this novel design did not perform positioning, the sensing technique can potentially simplify the design of passive VLP systems.

C. Wall Mounted Light Sensors

Localization is deduced from the change a target creates in the RSS of the ambient light measured by lightsensors embedded in the wall. Watchers on the wall (WoW) [43] uses the change in RSS at wall-mounted light sensors as a fingerprint and the weighted k-nearest neighbor (WKNN) classifier for positioning. The prototype system is able to track both a stationary and a moving target within a 2 m $\times$ 3.6 m area using 14 wall-mounted light sensors with median errors of 0.07 and 0.12 m, respectively. The work is an extension of Faulkner *et al.*'s proof of concept, Smart Wall, [54]. The same light sensors are utilized by Konings *et al.* [45] to develop FieldLight. It uses the change in RSS caused by a roaming target to localize. However, rather than using a fingerprint approach, FieldLight localizes by modelling artificial potential fields [55] attached to the light sensors that get triggered by the target when the measured RSS change exceeds a predefined threshold. Experiments conducted in three environments (7 m $\times$ 8 m foyer, 4.8 m $\times$ 9.6 m office, and 7 m $\times$ 4 m corridor) show median errors of 1.2 m, 0.84, and 0.68 m, respectively. In a "same environment" benchmarking at the office location, the FieldLight is found to be more accurate than a state-of-the-art DFL system that uses RF sensing [56].

It should be noted that passive visible light-based techniques are also being investigated for gesture recognition than can be useful for HCI. We would steer the interested readers toward the recent works reported in [57]–[61].

III. DFL With Infrared Sensing

PIR sensors are most commonly employed for localization based on IR sensing. A PIR sensor measures the IR radiation from a warm target (e.g., a human) within its FoV. These sensors are widely used as motion detectors for security alarms, automatic lighting, etc. Therefore, preexisting sensors can potentially be leveraged for localization purposes. In contrast to VLP systems, the IR-based systems can work under any illumination condition. It should be noted that the human target is the source of IR radiation. Therefore, while IR-based positioning is device free, the objective is to localize the source of the signal, not the "agent of change." One of the earliest examples of passive positioning using PIR sensors is reported in [62]. Lee *et al.* demonstrated the potential for positioning with the aid of simulation and some experimentation with three PIR sensors. There are many subsequent reported works [63]–[88] that have utilized PIR sensors for passive positioning.

The working of a typical PIR sensor is shown in Fig. 3. The two pyroelectric sensing elements are housed in their respective slots separated by a small gap. The elements convert the thermal energy received from the incident IR into electricity [89]. An IR emitting target entering the sensor's FoV activates the two sensing elements with a time delay, causing alternate positive and negative peaks. The elements are connected to the opposite inputs of a differential amplifier. Due to common mode rejection, only the contribution from the moving target is retained while that of the static ambience is canceled. Therefore, PIR sensors have inherent difficulty with stationary targets. The sensor's Fresnel lens, which is constructed from a number of lenslets, focuses the IR emission on the sensing elements, helps control the number of zones, range, and angle of coverage [89] and plays a key role in positioning. By using custom designed Fresnel lenses along with masks and by organizing multiple sensors in array

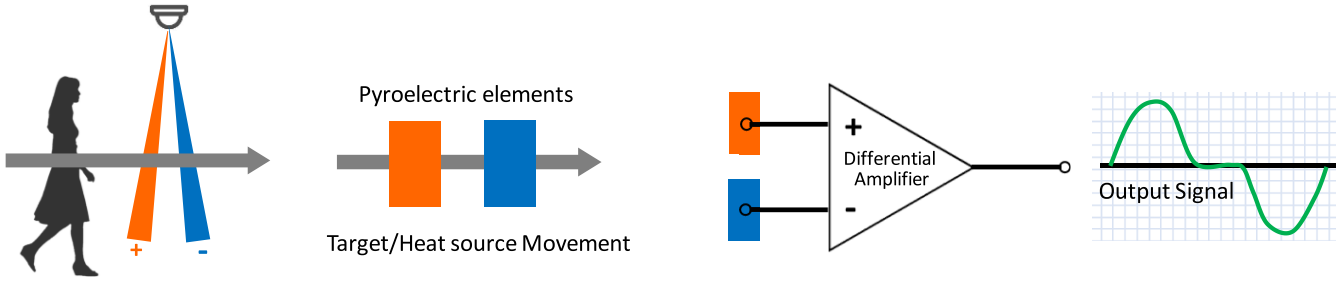

Fig. 3. Working principle of PIR motion detector.

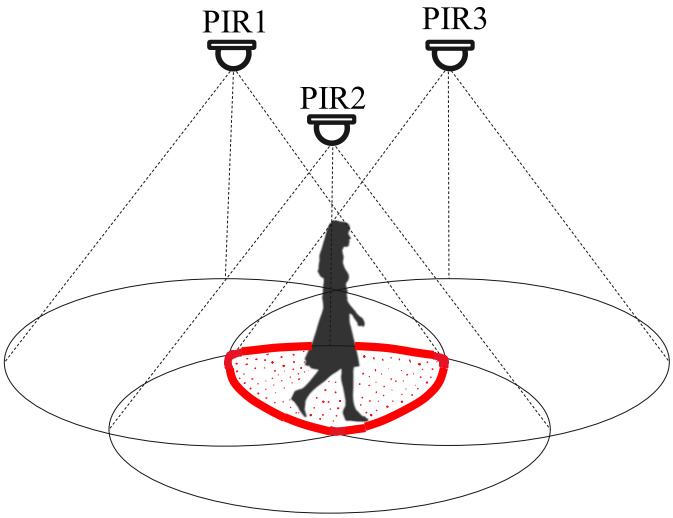

Fig. 4. Localization of target within the intersection of the triggered PIR sensors.

configuration, the detection regions can be made quite fine grained.

A. Localizing With Binary PIR Sensors

The basic principle of PIR sensor-based positioning is shown in Fig. 4. A sensor generates binary information indicating the presence/absence of a target within its detection zone. With the deployment of several sensors with overlapping coverage, the target can be localized within the intersection of the detection zones of the triggered sensors. Song *et al.* [63] reported the development of such a region-based positioning system. They deploy six ceiling mounted sensors in a 10.5 m × 6.6 m room, dividing it into 13 different regions. They demonstrate that it is possible to track a moving target and localize it accurately to the correct region, resulting in a maximum error of 5.25 m, as defined by the dimensions of the distinct regions. Most of the reported works using PIR sensor-based localization start with this basic concept.

Kim *et al.* [64] used ceiling mounted PIR sensors with overlapping coverage. They install 12 PIR sensors on the 2.5 m high ceiling of a 4 m × 4 m test area. The earlier version of the system performed coarse localization. If only one sensor produced an on signal, the target is localized to be directly underneath sensor. If the outputs of two adjacent sensors were on, the target's location was assumed to be at a point midway between the two sensors. If three or more sensors were on, the target was positioned at the centroid of the location of the corresponding sensors. They improve the localization by defining three output classes for the PIR sensors: inside, boundary, and outside of the sensing area and then using a Bayesian classifier. They conduct three experiments with targets between 1.6–1.8-m tall, moving at speeds of 1.9 km/h (slow steps), 2.6 km/h (normal steps), and 4.0 km/h (rapid steps). While they do not report any explicit statistic about the localization error, the accuracy of "about 0.8–0.9 m" and about "0.2–0.3 m" is quoted for the coarse and the refined algorithm.

Hao *et al.* [65] developed and implemented a prototype system for tracking multiple targets. Their system utilizes sensor nodes made up of a 2 × 4 array of binary PIR sensors whose FoVs are controlled by Fresnel lens arrays and coded masks to produce "type I" and "type II" sensors, respectively. Each node achieve a coverage of 144° with 14 detection zones covering an average of 10° each. The prototype system consists of four nodes deployed in a 9 m × 9 m room (each node at the midpoint of each side). The algorithm utilizes expectation-maximization scheme to determine the number of targets and positioning and then subsequent Bayesian tracking. The experimental results demonstrate simultaneous tracking of two targets in both "follow-up" and "crossover" scenarios with mean errors of less than 0.5 m. Their succeeding work with a distributive approach improves the scalability for large-scale deployment [66].

Jing *et al.* [69] reported a proof of concept that tracks a walking target in a lobby for two scenarios. In their "nonoverlapping" situation, six sensors are installed in a line on the ceiling. Two subjects, one at a time, follow a linear trace directly underneath the sensors. They estimate the walking speed (assumed constant) based on the time it takes for two consecutive sensors to turn on. Thus, assuming a linear trajectory, they are able to track the target. The mean error was found to be 0.394 and 0.35 m for the two targets. In the "overlapping" situation, they use 12 sensors on a rectangular grid and the target walk along predefined trajectories (not just straight lines). With the aid of Kalman filter-based tracking, the mean error for different trajectories vary from 0.595 to 0.926 m.

Sioutis and Tan [70] utilized space subdivision. Their sensor node consists of a cluster of seven sensors housed in a 3-D printed pod. They install three nodes on the 2.4 m high ceiling of a 5 m × 4 m room. The room is thus divided into 700–850 unique areas, with each covered by a unique combination of sensors. Position is estimated by evaluating the state of the sensors. Four different trajectories connecting six points are traversed by the target, briefly pausing at some locations while

walking past others. While the localization accuracy is not explicitly given, the authors surmise the positional error to be less than 0.5 m.

Yin *et al.* [77] tracked the room-level movement of two residents living in a smart home outfitted with five motion sensors. The data from the sensors are collected for a year while the two occupants followed their normal daily routines to develop naïve Bayes and hidden Markov model (HMM) location estimators. The performance of the developed algorithms is evaluated over a one-week period, when the participants wore Bluetooth tags to produce ground truth (GT). The accuracy of both estimators is found to be approximately 73% in identifying the room the target is located in.

Luo *et al.* [79], [80] implemented a system with five ceiling mounted sensor nodes placed on the four corners and the center of a 4 m $\times$ 4 m square. Each node consists of nine PIR sensors arranged in a 3 $\times$ 3 grid providing 40 fine-grained radial detection zones through the use of two types of masks doing radial and bearing segmentations. The region-based target location is initially [79] refined by a Kalman filter and a Kalman smoother. They conduct experiments in an office environment with the target tracing four routes along a 3 m $\times$ 3 m rectangle (one side, the perimeter, the diagonal, and side-diagonal-side-diagonal) at various walking speeds. The average RMSE is about 0.6 m. In a follow up article [80], they apply a two-layer random forest classifier for both tracking and activity recognition. The mean accuracy while classifying among five common daily activities is reported to be better than 92%. The mean positioning error is 0.85 m.

Yang *et al.* [82] proposed refining the coarse, zone-based localization by utilizing an accessibility map and the A-star algorithm. Ten narrow FoV PIR sensors are installed in a 12 m $\times$ 7.2 m mock apartment. During the calibration period, an accessibility map of the apartment is developed as a heatmap with 0.1 m $\times$ 0.1 m grid based on the number of times the occupant visits the respective grid nodes during daily activities. The beginning of a route is taken as the start node of the A-star algorithm. At any given time, the current node is the location of the target. Eight candidate nodes are selected around the current node. The goal node is given by the grid point with the maximum heat score within the triggered sensor's detection zone. The target node is determined by a cost heuristic function. For two investigated routes, the mean localization error was found to be 0.21 m, which is comparable to the accuracy of the method reported by Kim *et al.* [64] but with a significantly sparser sensor deployment density.

Yang *et al.* [85] employed a mesh network of PIR sensors for tracking multiple targets. The sensors are equipped with a special lens that allows each sensor to have six overlapping detection zones. Each zone is represented by a "detection line" and if a target is detected within a zone, it is assumed to be on the corresponding detection line. The intersections of all the activated detection lines are candidate target locations. This bearing crossing algorithm for target positioning is further refined through K-means clustering and then a Kalman filter is applied to track the moving target. The experimental results with nine sensors produce mean tracking error of less than 0.8 m in a 10 m $\times$ 10 m space with two human targets walking along several trajectories. This is an improvement of their earlier works reported in [72], [75], and [76].

The localization performance of a PIR sensor-based system, like any others, depends on the placement of the sensors. Vlasenko *et al.* [71] and Fanti *et al.* [90] discussed the optimum placement of the PIR sensors and developed optimization algorithms that consider various practical constraints (e.g., number of sensors, obstacles such as tall furniture, etc.).

B. Localizing With Analog Voltage Output of PIR Sensors

The works discussed so far have used the PIR sensors primarily as binary sensors (which is the typical mode of operation of common motion sensors). However, a PIR sensor generates a voltage signal proportional to the change in IR radiation received by the pyroelectric sensors. This raw voltage level is then converted to a binary value by comparing it to a predefined threshold. It stands to reason that this hard thresholding leads to some loss of information. Therefore, several works [67], [68], [74], [78], [81], [83], [86], [87] have used the raw, analog output of the sensors for localization purposes. By exploiting the more information rich raw output from the sensors, these solutions can localize with a smaller number of sensors compared to the binary sensor-based systems. Many of these works create parametric models linking the distance of the target from the sensor and the raw output of the sensor.

Zappi *et al.* [67] extracted features from the analog output of a pair of PIR sensors, termed as clusters, to track people. Each sensor of a cluster is mounted facing each other on opposite walls of a 2.5 m wide hallway. The space between the two sensors is divided into three regions: 1) close to sensor 1 (within 0.8 m of sensor 1); 2) middle (stretch of 0.9 m in the middle); and 3) close to sensor 2 (within 0.8 m of sensor 2). In their experiments, they use three clusters along the hallway and record 200 passages of each class. The target is localized to one of these three regions under a cluster using a classifier. They are able to detect direction of movement with 100% accuracy. The accuracy of correctly identifying the location of the target within the three classes for naïve Bayes, support vector machine (SVM), and K-nearest neighbor (KNN) classifiers, are 83.49%, 87.5%, and 95.35%, respectively. This work builds on [91] where features were extracted from three sensors to estimate the direction of a target's movement and also to count the number of targets.

Monaci and Pandharipande [68] observed that the sign of the output voltage of a triggered PIR sensor can indicate the direction of the target's motion with respect to the sensor. They also find that when the detection regions of a pair of sensors partially overlap, it is possible to associate their corresponding signal levels to spatial zones. In their DFL system, each triggered sensor quantizes its analog output with two predefined thresholds. The ternary outputs from a pair of sensors with overlapped detection regions are then used to determine the occupancy within a fine-grained spatial zone. However, the localization is highly sensitive to the threshold levels and quantization steps. HMM is used to deal with the inaccuracies arising from incorrect thresholding by characterizing the transition of spatial zone occupancy, with each zone representing a discrete state. A maximum-likelihood sequence estimator

(MLSE) determines zone occupancy and tracks the target. The performance of the system for 1-D zoning and tracking is evaluated in a 6.4 m × 3.7 m space with two sensors. For the four simple trajectories investigated, the system is able to locate and follow the target correctly across the zones.

Narayana *et al.* [74] argued that an array of multiple collocated PIR sensors is more robust to false/low detection compared to a network of distributed sensors. They construct a tower housing two sets of four sensors and use their analog outputs for localization. They develop a model relating the distance of the target from the sensor to its peak-to-peak output voltage. The distance of the target from a sensor is estimated through zoning. This ranging involves forming detection zones for each sensor in the array by having different gains for each to make them output maximum peak-to-peak voltage at different distances. Two towers are deployed on 1 m high tripods at 90° angles with respect to each other at the ends of the hypotenuse of a right-angle triangle with legs of 4 m. The center of the coverage of each tower coincides with the respective legs. They report localization error of 0.2 and 0.6 m for less than 5 and 10 m ranges, respectively, in a large classroom with desks and other furniture. The system can also be configured to classify the height/width of the moving target.

Mukhopadhyay *et al.* [81] also used a calibrated model that relates the peak-to-peak output voltage of the sensor to its distance from the target. Of the two ranging techniques developed from the parametric model presented in their earlier work [89], the piecewise linear one is found to be more accurate. Ranging is followed by localization using multilateration and support vector regression (SVR). Their experimental setup consists of four sensors, which are time synchronized, deployed in a 7 m × 7.5 m area. The localization RMSE for 40 test points is found to be 0.65 and 0.85 m for SVR and multilateration, respectively. For the same setup, the RMSE of Narayana *et al.*'s method [74] is 1.2 m.

Liu *et al.* [86] used the "azimuth change" extracted from the raw output for positioning. They define the azimuth change as the absolute difference of the azimuth of the target with respect to a sensor at two locations. The extraction is based on modeling the PIR sensor as a second-order dynamic system whose parameters depend on its physical properties. The obtained azimuth change information is used to build the observation model of a particle filter that tracks the moving target. Their prototype deployment has four sensors located at the corners of a 7 m × 7 m open space. The target takes roundtrips along six predefined traces five times each. The mean localization errors are between 0.47 (straight line trace) and 0.71 m ("horizontal snake-like curve") resulting in an overall mean error of 0.63 m. The 80-percentile error is less than a meter for all six cases. They investigate the impact of the number of sensors and find the mean localization errors to be 2.5, 1.7, and 0.9 m for one, two, and three sensors, respectively. They also show that their system is more accurate in correctly localizing a target within a 1 m × 1 m grid compared to what Narayana *et al.* [74] achieved in a comparable scenario.

Yang *et al.* [87] argued that the relationship between the sensor's analog output and location of multiple targets is extremely complex and difficult to model. Therefore, they propose a deep neural network (DNN)-based approach for localizing multiple targets. They assume that the response of sensors at the presence of multiple targets can be approximated by the superposition of response to each target and additive noise. Their DNN, termed PIRNet, therefore, consists of two modules. The first module demixes the signal and determines the number of targets. The other module extracts features and localizes the individual targets. Rather than giving the raw sensor outputs to the NN directly, they use signal processing and data augmentation to preprocess the data. They achieve mean localization errors of 0.43, 0.6, and 0.82 m for one, two, and three simultaneous targets, respectively, in a 7 m × 7 m open space covered by four sensors. The PIR sensors used for this work appear to be the same as those used by Liu *et al.* [86].

Li *et al.* [78] specifically address the inability of PIR sensors to handle a stationary target by making the sensors rotate to create relative motion between the sensor and the target. Their sensing module is a turntable tower equipped with 16 narrow FoV sensors and a DC-motor for rotation. They report an "accuracy" of 0.113 m while tracking a target following a pricewise linear "snake-like" trajectory in a test area of 6 m × 6 m equipped with two sensing towers.

Wu *et al.* [83] utilized a semitransparent rotating shutter, driven by a stepper motor, to create nonlinear IR flow into a 2 × 2 PIR sensor array to detect and localize a stationary target. The peak-to-peak output voltage and "intersections points," where the voltage signals between the two peaks meet with the half of the supply voltage, are used as the features for ML classifiers that perform zone level localization. The sensor node is ceiling mounted at a height of 2.8 m. It has 12 radial segments of coverage zones with radial distances of 1 and 2 m and angular separation of 60°. The accuracy of the four supervised classifiers, namely, the SVM, KNN, naïve Bayes and decision trees, in identifying the target within the correct zone are found to be within 97.47%–98.89%. The duty cycle of the output is found to be an effective feature for detecting whether the target has a side facing or front/back direction. The relatively high power consumption of the stepper motor is a significant drawback of this scheme. A low-power alternative using an electromechanical vibrator to drive the shutter is presented in a subsequent work [92].

C. Localizing With Thermopile Sensors

Thermopile sensors are typically constructed from series-connected thermocouples for sensing the IR radiation [93]. In contrast to PIR sensors, they measure the total amount of the incident IR flux, not its change. Therefore, they are able to detect a stationary target also. They are commonly used for contactless temperature measurement in microwave ovens, cooktops, air conditioners, thermometers, etc. Passive human positioning based on thermopile sensing has been reported in [94]–[101]. Other than Kemper and Hauschildt [94] who propose to use bespoke line sensors, the reported works utilize commercially available thermopile array/grid sensors (the 8 × 8 Panasonic Grid-Eye being the most popular choice), which are essentially very low-resolution thermal cameras. The basic concept of thermopile-based sensing of a target is illustrated in Fig. 5. The thermal image is privacy preserving

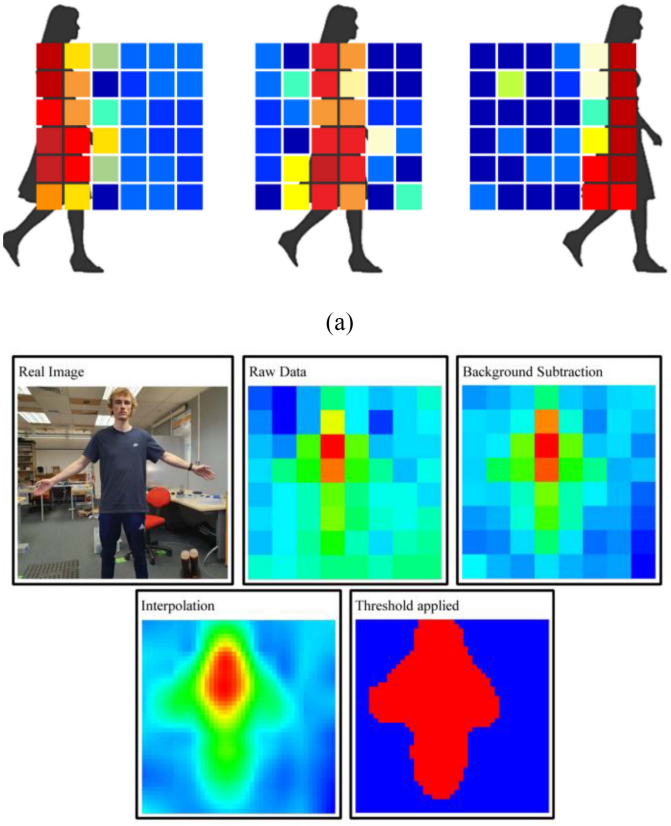

Fig. 5. (a) Illustration of localization with thermopile array. (b) Example of typical image processing of heat signature captured by a thermopile with one of the authors standing in front of a Panasonic Grid-Eye.

as it does not contain any identifiable information. The application of image processing techniques, such as background subtraction and noise reduction (through averaging or filtering), can improve the quality of the thermal image of the target followed by blob detection to infer the presence of the target. Parametric model (e.g., heat-distance relationship) calibration can also be applied for estimating depth or range.

Hevesi *et al.* [97] reported tracking with "an accuracy in the range of 1 m" using a ceiling mounted 8×8 array. However, the emphasis of the work is more on activity recognition. Basu and Rowe [98] discussed the utilization of the IR image captured from a ceiling-mounted thermopile array for people counting (up to four) using SVM classification and identifying the direction of motion using normalized cross-correlation between the time series of the pair of pixels. While they do not perform explicit positioning, the image processing techniques utilized for feature extraction can be quite useful for localization. Thermopile sensors have also been used for occupancy detection [102], fall detection [103], activity recognition [104], respiratory flow monitoring [105], pose detection [106], etc.

Kuki *et al.* [95] tracked human movement by capturing the thermal image with a ceiling mounted 4×4 array. The pixels associated with the target are detected after background removal using three "if-then" fuzzy rules on sensed temperature. The target pixels are then used to define the target area by blob detection. The polygon that connects the centroid of each blob is the target trajectory. For their experimental setup, the sensor is installed 2.73 m off the floor. A 1.58 m $\times$ 1.58 m area underneath the sensor is the monitored zone. They track a target performing 15 different motion patterns that include walking at various speeds, crawling, etc., within 0.396 m $\times$ 0.396 m zones. They report a mean positioning error of 0.215 m. They later extend the work to count people [107] and coarse positioning of multiple targets [108].

Ng [96] localized using a network of wall-mounted thermopile sensors. He assumes that the output of a thermopile is related to the amount of incident IR. Therefore, if the temperature and area of the sensed target are constants, the distance of the target from the sensor can be estimated from the detected temperature. Temperature–distance calibration curves are derived for front and side-facing poses. Five sensors are installed on two perpendicular walls of a 4.6 m $\times$ 2.7 m room (three on the longer wall or along the vertical axis with the remaining two along the horizontal axis). The positioning along each dimension is achieved by finding the distance corresponding to the highest temperature between the sensors along that axis. The positioning accuracy, presumably mean error, for a simple horizontal and a vertical trajectory is found to be within 0.5 m. He also accurately identifies common human activities, such as walking past a doorway, lingering outside, or entering a room.

Chen and Ma [99] localized by extracting the Angle-of-Arrival (AoA) information from two wall-mounted, time-synchronized 16×4 sensors. Noise reduction through multiframe averaging and then background subtraction is utilized to detect the target from the IR image. The position derived from AoA is further refined using a quadratic regression model. They monitor a 3 m $\times$ 2.35 m area with two sensors that are 3.3 m apart, installed at a height of 1.2 m. The mean positioning error for a "snake-like" trajectory is 0.1339 m. They also implement fall detection using a KNN classifier.

Shetty *et al.* [109] utilized an 8×8 array for target detection with Kalman filter-based tracking. They use bicubic interpolation to enhance the thermal image and then perform background subtraction. The extracted foreground is then denoised with a Gaussian filter. This is followed by binary thresholding and blob detection. The centroid of the blob, representing the target position, is tracked using the Kalman filter. While they do some initial testing to demonstrate a proof of concept, no localization experiments are conducted, and no positioning accuracy is reported.

Chen *et al.* [100] classified target facing direction using an 8×8 sensor. The raw IR images from the array are processed by applying background subtraction followed by linear interpolation and thresholding to create 32×32 binary matrices. They utilize the convolutional neural network (CNN) to extract features from these binary matrices to train an SVM classifier. By integrating the array with a Time-of-Flight (ToF) distance sensor on a rotational target tracking platform, they are able to achieve 0.19 m localization RMSE. The experiments are conducted within a 1.2 m $\times$ 2.4 m rectangular area. The platform is placed in the middle of one of the longer sides and the target walks back and forth along the remaining three sides.

Kowlaski *et al.* [101] utilized wall-mounted sensor clusters consisting of three 8 × 8 thermopile arrays mounted in a custom-designed 3-D printed case. They employ two clusters to cover a 2 m × 2.5 m area divided into twenty 0.5 m × 0.5 m cells. The sensor clusters are attached to the middle of two perpendicular walls at a height of approximately 1.5 m. SVM is used as the classifier to position the target within a cell based on the feature vector consisting of the temperature values registered at the sensor clusters. They collect 2128 samples and train the classifier with 75% of this data. For the remaining 25% data, the accuracy of the classification for positioning within a single cell and within a neighborhood of four cells is 73.1% and 93%, respectively.

Qu *et al.* [110] formed temperature and shape signatures (to eliminate nonhuman heat sources) from the IR image captured from a wall-mounted 8 × 8 array. Interpolation is used to create a 71 × 71 image which is smoothened or denoised by Gaussian filtering. Adaptive thresholding, making all pixels lower than the threshold to be equal to the threshold, is then used to eliminate the background. The pixel with the highest temperature corresponds to the relative location of the target in the sensor array, which is then converted to actual location by using a parametric model. The system tracks target using a Kalman filter. In a 4 m × 4 m area with the target walking along the diagonal, the mean localization error is found to be 0.07 m. The system can track multiple targets (up to 3) simultaneously by data association through "energy characteristics." This exploits the fact that humans having different shapes and clothes produce different heat signatures that cannot change markedly within the detection period. While the accuracy degrades, the system can track all three targets even for cross-walking where the targets come together and then diverge.

Narayana *et al.* [88] proposed a fusion of PIR and thermopile sensors for positioning. Their earlier work [74] is leveraged and improved upon to develop a parametric model linking the analog output of the PIR sensor to the target's distance, speed and direction. The PIR sensor acts a depth sensor providing an estimate of the range between the sensor and the target. Once a presence is detected by the PIR sensor, a collocated 32 × 24 thermopile array captures the thermal image to provide an estimate of the target's location in the other two dimensions: 1) across the FoV cone axis and 2) the height of the object. Thus, a single sensor node (termed FOCI) can localize the target by using a KNN classifier to match the pair of information from the two sensors. It should be noted that background subtraction and Gaussian filtering along with interpolation are used to improve the thermal image. For their experimental setup, a single FOCI sensor is mounted at a height of 1.2 m to monitor a 9 m × 8 m area. Training and calibration data are collected from 20 different individuals wearing different types of clothing on different days and walking at different speeds. For testing, ten targets (one at a time) walk randomly at various speeds. Twenty recordings for each target are taken. The median and 80-percentile error are 0.22 and 0.35 m, respectively. For multitarget tracking with two and three subjects, 82-percentile error of 0.88 m is achieved.

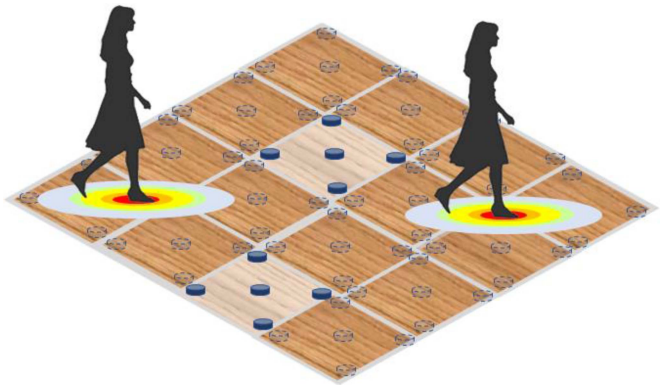

Fig. 6. Positioning on a pressure sensitive floor by localizing the center of pressure. Pressure sensors (e.g., load cells) are embedded underneath floor panels.

We also noted a DFL system that employs IR cameras capturing the reflection of signal transmitted by IR LEDs mounted on those cameras from retroreflectors fixed on the walls [111]. The positioning is inferred from the occlusion created by the target passing between the camera and the reflectors. Santo *et al.* reported a mean localization error of approximately 0.3 m with two cameras deployed in three experimental setups in rooms with dimension of 3 m × 3 m, 4 m × 5.5 m, and 4 m × 7 m, respectively. While the system is technically privacy preserving (no image of the target is captured), it may not be perceived as such. In fact, the authors themselves mention the need for investigating its acceptability since the IR camera looks similar to a normal RGB camera.

IV. DFL by Localizing Physical Excitation Source

Whenever a person moves around indoors, they contact the floor with each step that they take. Each footstep can be thought of as the source of a physical excitation. The positioning of the person can be achieved by locating the source of the excitation, i.e., the footstep. Therefore, while the target is untagged, the (footstep) positioning is equivalent to localization of a source.

A. Pressure Sensitive Floor

Floor embedded with piezo-electric/resistive pressure sensors is one of the oldest reported techniques for locating and identifying people. Such pressure sensitive floors are able to sense the force at which a subject's foot hits the ground and can identify individuals by analyzing the ground reaction force (GRF) [112]. Pressure sensitive floors can be constructed from small panels supported by load cells as shown in Fig. 6. Early examples of such floors are the ORL Active Floor [113] and the Smart Floor [114]. Other alternatives include force sensing resistor (FSR) [115], grid of piezo electric wires [116], electro-mechanical film [117], piezoresistive carbon granules mixed with rubber [118], etc.

Liau *et al.* [119] constructed a floor from 0.6 m × 0.6 m blocks with embedded load cell in the middle. Twenty-five blocks separated by 0.2 m are installed underneath a regular wooden floor in a 5 × 5 grid. They utilize a Kalman

filter-based algorithm, probabilistic data association (PDA), to track the target. This is augmented with LeZi-Update to handle cross-walking for the multitarget scenario. Personal profiles for individual users are created based on their respective GRF. The 85-percentile error while tracking a single target tracing the perimeter of a 2.4 m $\times$ 1.6 m rectangle is 0.2828 m. While tracking two targets with significantly dissimilar weights with one following the rectangular path while the other walking randomly around a small area, the localization error of 0.2828 m is observed at the 76.25-percentile. Even though they track two targets moving on linear cross-walking trajectories, localization accuracy for that scenario is not reported.

Andries *et al.* [120] installed a floor constructed from a network of 104 tiles in a mock apartment. Each 0.6 m $\times$ 0.6 m tile has load cells underneath its four corners. The data acquisition is done using the "smart tiles platform" introduced in [121]. They apply computer vision techniques by treating the load values read from the floor analogous to the light-intensity bitmap image generated by the image sensor of a camera, respectively. Blob detection, where the blob is created by the target exerting force at the load sensors, is performed followed by localization and tracking of the blob. Background subtraction is applied to remove the contribution from other sources like furniture etc. They initially track a wheeled robot doing a figure of eight loop (approximately 2.5 m $\times$ 1 m) and obtain a mean localization error of 0.08 m. For a human target, the center of pressure of the blob is taken as the position of the target. They report a mean error of 0.13 m for a human going through a "morning routine scenario." Large errors (1.5–2 m) occur when the target is close to heavy furniture. For a two-target "receiving a visitor" scenario, the mean error is 0.2 m. In this situation, the large errors occur when the two individuals are in close proximity, occupying a contiguous space in terms of tiles. Daher *et al.* [122] used the same floor for activity and fall detection. Data from an accelerometer, located at the center of each tile, are fused to improve the fall detection performance.

Al-Naimi and Wong [123] used sensing units constructed of 16 FSR sensors arranged in a 4 $\times$ 4 array within a 0.5 m $\times$ 0.5 m plywood. The testbed has 16 sensing units covering a 2 m $\times$ 2 m space. The localization algorithm first segments each footstep and identifies the cluster of contiguous sensors (maximum of six due to the geometry of the layout and the size of a human foot) activated by each footstep. Each sensor is triggered at a slightly different time depending on when they come in contact with the foot. A pattern signal for each footstep is generated by combining the time delayed voltage signals. The centroid of this pattern represents the footstep's centroid. The mean footstep localization error for a single target on straight and curved trajectories is 0.0767 m based on 120 footstep data collected for each case during experiments.

Murakita *et al.* [124] used 0.18 m $\times$ 0.18 m binary pressure sensors to cover a 37 m^2 testbed. They consider the output of the sensors forming binary images. A particle filter is applied with both a linear Gaussian and a nonlinear bipedal prediction model for tracking. The bipedal model is more accurate but is found to have more difficulty discriminating between multiple subjects. Ten targets walked a marked 30 m test course three times each. A mean error of 0.2 m is achieved with a maximum error of 0.59 m. The system can discriminate between two targets at 90% accuracy if they remain at least 0.8 m apart.

Lan *et al.* [125] utilized compressive sensing with multilayer binary pressure sensors, where each layer of the pressure sensors is constructed from sponges sandwiched by two tin foils. The sponge layers have holes through which the two foil layers can come into contact when pressed by a subject's footstep creating an electrical connection generating a 1-b output "1" for the corresponding layer. The observation space is divided into multiple zones with each being encoded with a binary code. Target detection and localization are treated as encoding and decoding, respectively. A space encoding scheme based on low density parity check matrices is utilized with the decoding being performed using Bayesian inference. The testbed consists of 3.6 m $\times$ 3.6 m area covered by six-layer binary pressure sensors organized in 36 zones as a 6 $\times$ 6 grid. They perform multiple experiments with 1–4 targets and accomplish grid level localization in real time. The localization accuracy is better than 80% for up to three targets and it comes down to 50% for four targets indicating the need for a denser sensor grid. This a continuation of their earlier work [126], where they developed the detection and the localization algorithms.

Many works (e.g., [113]–[118] and [127]–[129]) use pressure-based flooring similar to the ones discussed in this section for activity detection, fall detection, and target identification. "Intelligent carpet" using plastic optical fiber (POF) sensors [130] has also been proposed for footstep imaging. If used in an appropriate manner, these systems can potentially be used for localization.

B. Vibration Sensing

The basic idea of vibration-based localization is illustrated in Fig. 7. The floor or structural vibrations induced by the target's footsteps are measured with geophones or seismic sensors. The footstep event is identified apart from other excitation events (e.g., fall of a chair), typically with a classifier. With a network of distributed sensors registering the vibration signals resulting from the same footstep at different times, a TDoA algorithm can localize the excitation source, the footstep. It should be noted that since the origin time of the footstep is not known *a priori*, ToA cannot be used for localization purposes. Also, vibration waves propagating through a structure like floor experience exponential attenuation with distance. Therefore, the error of RSS-based range estimation has an exponential relationship with distance. In contrast, TDoA ranging error is linearly proportional to arrival time estimation making it more suitable for this scenario [131]. Vibration-based localization has synergy with and can build on the techniques used for active source localization within other bodies of research. However, the floor is a complex and heterogenous propagation medium compared to air, water, and free-space RF. One of the advantages of vibration-based DFL is that it may be able to leverage preexisting sensors

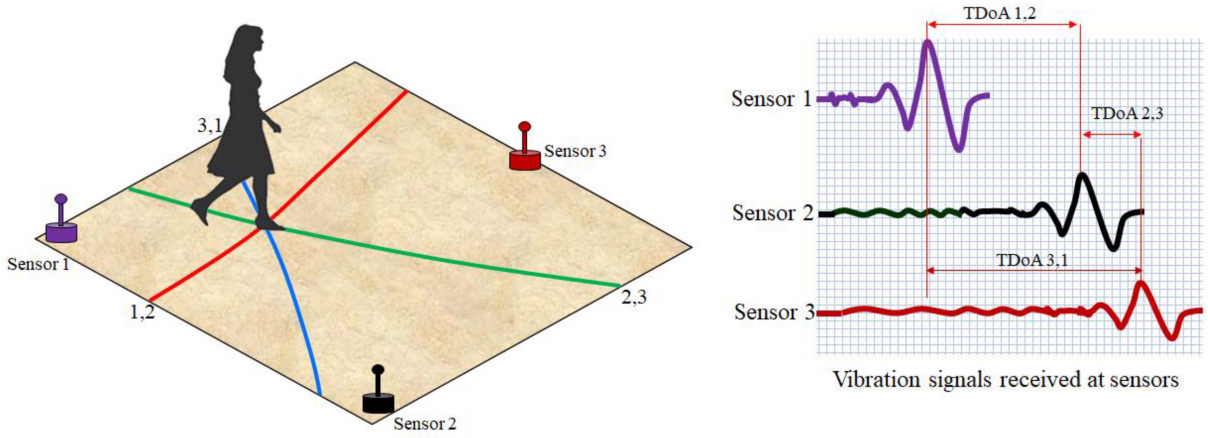

Fig. 7. Vibration-based positioning. The target is localized at the intersection of TDoA hyperbolas.

that are part of the structural health monitoring system of the building [132].

Floc [133] is a footstep localization prototype that utilizes p-wave geophone sensors. Chen *et al.* found that the ambient noise mainly manifests at lower than 63 Hz and they remove that with a high-pass Butterworth filter. A calibrated mathematical model is developed to detect footsteps with a reported 97% accuracy. After detection, the corresponding footstep is localized using TDoA. A proof of concept experiment is conducted in a 6 m $\times$ 8 m cluttered office. Three geophones are installed on the floor at the vertices of a right-angle triangle (legs of 4 and 3 m). Three subjects (one at a time) take three steps within this triangular space 20 times each. A mean localization error of 0.07 m is achieved.

Bahroun *et al.* [134] theorized and experimentally demonstrate that the propagation velocity of the vibration wave in a bounded medium like a concrete slab is a function of the source-sensor separation. This makes range estimation, therefore algorithms like TDoA, subject to measurement error. They propose localization using the sign of TDoA instead. This capitalizes on the observation that even with varying propagation velocity, the order at which the vibration waves arrive at the sensors does not change; further distance still results in higher propagation time. The sign of the arrival time between a pair of sensors is used to define a zone of possible location of the footstep. If the space between a pair of sensors is divided by a perpendicular bisector of the line joining the pair, the source will be on the side of the sensor that receives the vibration signal earlier (positive sign of TDoA). Multiple such zones created from multiple pairs of sensors and known boundaries (like walls) localize the target. They conduct proof of concept experiment with nine seismic sensors arranged as a 3×3 grid in a 3.6 m $\times$ 5.4 m space on a 0.2 m concrete slab covered by a tiled floor. For seven footsteps, they report positional errors between 0.29 and 0.68 m.

Mirshekari *et al.* [135] used an SVM classifier to identify the footstep event followed by localization utilizing TDoA. Since a vibration wave is dispersive in nature having multiple frequency components with different velocities, the algorithm uses signal decomposition to group components with similar propagation characteristics. Since the floor is a heterogenous medium, the propagation velocities also depend on the location. An adaptive multilateration based on heuristics mitigates this by constraining the search space. The algorithm requires a minimum of four sensors for localization. Experiments are conducted in three different locations with three individuals (one at a time) walking multiple traces at various walking speeds within a 5 m $\times$ 4 m space. They conclude that when the footstep is within a polygon formed by the sensors, the localization accuracy improves. An overall median localization error of 0.38 m is achieved. The localization accuracy can be traded off with the number of deployed sensors. Further refinement is proposed in [136] by using a model transfer approach to improve footstep detection. They project the data into a feature space in which the structural effects are minimized for more robust detection. This research group has published several other synergistic works that characterize the vibration wave propagation [137], perform occupancy detection [138], fall detection [139], target identification [140], occupancy traffic estimation [141], etc.

Shi *et al.* [142] from the same research group report multiple target localization of three concurrent walkers. Since footsteps from multiple targets are not synchronized, only partial overlaps occur between vibration signals induced by concurrent walkers. Furthermore, stepping frequencies and walking patterns vary among individuals. Therefore, the heel strike timing for concurrent walkers may not be also completely overlapping. The footstep event detection is done with the raw vibration signal. They decompose the detected vibration signal using wavelet transformation, identify the number of targets and extract the onset of footstep signal (i.e., the heel strike). Each target is then localized independent of each other using TDoA. Experimental setup uses four geophones monitoring a 3 m $\times$ 4 m area. The localization is performed for three scenarios: 1) cross-walk; 2) side-by-side; and 3) follow (three steps away) with a mean localization error of 0.65 m.

Poston *et al.* [131] proposed a robust localization algorithm that takes the distortion experienced by the vibration wave propagating within a building's structure into consideration. In contrast to other works, they use preexisting sensors that

are already embedded as a part of the building's structural dynamics instrumentation. They classify two types of footsteps. The compression case when the footstep is directly over one of the sensors, the vibration waves experience little distortion; the location of the footstep is essentially that of the sensor. The rest of the footsteps are classified as the general case with wave distortion and the localization is performed using TDoA after footstep detection. The footstep detection is achieved with a matched filter, where the impulse response of the filter is constructed from representative excitation signals collected during the calibration process. Experiments are performed in a 25.5 m $\times$ 2 m corridor and a 15.8 m $\times$ 17.2 m lobby of a building. Both areas had 12 sensors. The localization RMSE with the target walking along linear trajectories are 0.6 and 0.8 m, respectively. This work is an extension of the preliminary efforts reported in [143]. Poston also extends the work [144] to account for two targets simultaneously by applying Kalman filtering and multiple hypothesis tracking.

Alajlouni and Tarazaga [145] developed a computationally simple algorithm based on heuristics and utilized the fact that sensors nearer to the footstep register higher energy compared to the distant ones. The simple peak detection algorithm is applied for footstep detection. The energy received at the sensor exceeding a predefined threshold and within a predefined time window ending at the peak of the detected vibration signal is computed. The footstep's position is the weighted average of the sensors' locations with the corresponding measured energy as the weight. The work is an extension of the concept reported in [146]. The testing is done in the same instrumented building that Poston *et al.* [131] experimented in. With the target following a linear trajectory back and forth along a 13 m $\times$ 2 m corridor, the 80-percentile localization error is 0.7 m.

Vibration-based localization is highly dependent on correctly identifying footstep-impact events from similar spurious events like objects falling. Low SNR due to ambient noise can also make the detection of footstep-induced floor-vibration signatures difficult. Drira *et al.* [147] developed an accurate classifier to identify footstep-impact event. After analyzing the event signals within a range of 10–260 Hz, they conclude that combining information from multiple frequency components is the key to accurate event identification. Also, using both low and high frequency components increases the accuracy of the classifiers. Another relevant study conducted by Lam *et al.* [148] suggests focusing on the vibration signal components around natural frequencies of the structure to increase the SNR. Vibration-based localization is also impacted by varying rigidities of structural floors, obstructions, variation of the signal due to shoe types, etc. Drira *et al.* [149] proposed using physics-based models in the interpretation of vibration measurements as an effective way to minimize these effects. While no localization is performed in these research works, the findings can help design more robust localization techniques.

V. DFL With Electric Field Sensing

Electric field sensing involves measuring the change in the capacitive coupling between the target and the objects present in the environment. In the literature, when a transmitter actively generates an electric field, with the target changing the field, it is commonly referred to as capacitive sensing. In contrast, the transmitterless sensing that measures changes in the ambient electric field by the target's presence and movement, is commonly termed as passive electric field sensing.

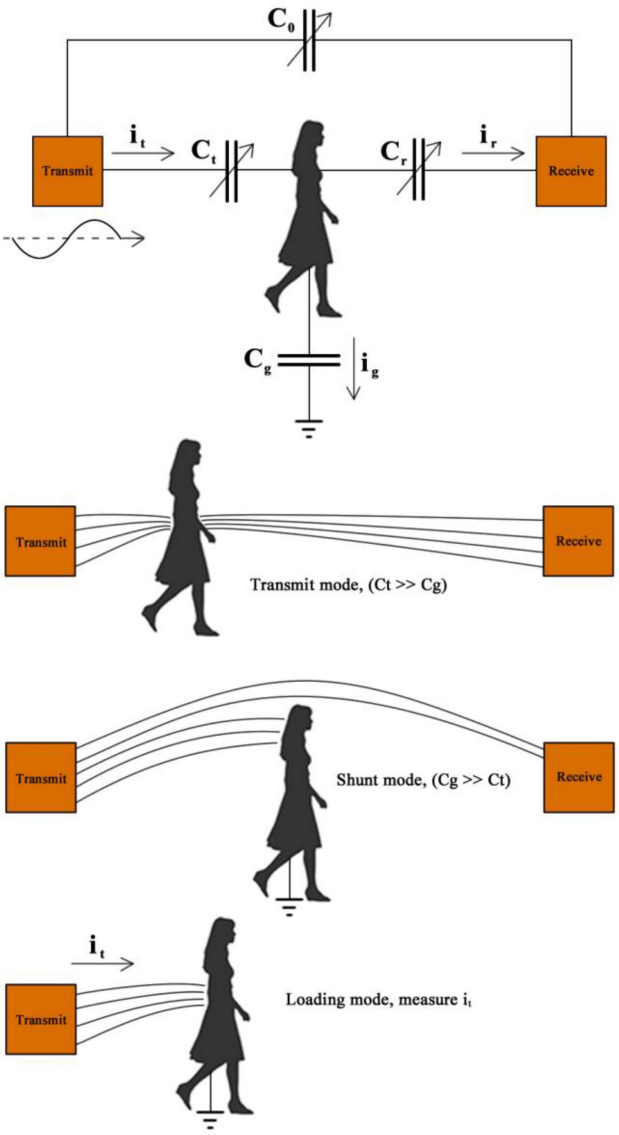

Fig. 8. Capacitive coupling and three modes of capacitive (active electric field) sensing.

A. Localization With Active Sensing

There are three sensing modes for active capacitive sensing as explained by Zimmerman *et al.* [150] and Smith *et al.* [151]: 1) transmit mode; 2) shunt mode; and 3) loading mode, as shown in Fig. 8. In the transmit mode, the signal from a transmitter is coupled by the subject's body, which then becomes an electric field emitter. This only happens when the target is very close to the transmitter and the body effectively becomes an extension of the transmitter. In the shunt mode, the target's body conducts a portion of the signal to ground. The remainder of the signal which is not blocked by the target can then be

measured at the receiver. This happens when the target is not close to either electrode. In loading mode, there is no receiver and the environment effectively forms the second plate of the capacitor to ground (Fig. 8). Loading mode capacitive sensing underpins the popular touchscreen technology and is also the most common mode of active sensing for localization.

Savio and Ludwig [152] developed the Smart Carpet, one of the earlier capacitive systems, using fabric with conductive wires sewn into it. The wires are formed into serpentine shapes to construct 0.15 m × 0.15 m panels that are used as the plate of a capacitor in loading mode. When a target's foot is in proximity to a panel, the measured capacitance increases. Predetermined thresholding is used to identify which plates have been activated by the target's footstep. Three different techniques are used to cluster the groups of squares associated with a single foot: 1) simple heuristics; 2) MLE; and 3) rank regression. The midpoints between successive footprints are used to estimate the trajectory. They implement a 2.4 m × 2 m prototype using 180 panels. Twenty-four test subjects (including children and adults of both genders) walked on multiple trajectories. The mean-square error (MSE) of localization is between 0.0187 (line) and 0.431 m (C-shape) for various trajectories. Lauterbach *et al.* [153], [154] developed another similar system, SensFloor, which uses conductive triangles embedded in a textile with a density of 32 triangles per m^2. As with the Smart Carpet, these triangles form the plate of the capacitor in loading mode. The floor is later used with hip-mounted accelerometers to identify individuals [155]. A Kalman filter is used to improve the tracking of people around the room and implement multiple subject tracking. However, the accuracy of the system is not quantified.

Rimminen *et al.* [156] were similarly able to track occupants in a room with conductive panels underneath the floor forming one plate of a capacitor whilst sensing in the loading mode. A floor of a 4 m × 4.5 m room is embedded with 0.25 m × 0.5 m sensor panels. A mean positioning error of 0.21 m is achieved while tracking a moving target. Multiple walking speeds are investigated, with smaller positioning error at lower speeds. As a person walks, the footsteps alternate from side to side, deviating from the subject's actual course. A Kalman filter is shown to perform better than simply tracking the centroids of successive footsteps. A particle filter is used for multiple target tracking. Two targets can be individually separated with 90% accuracy if they are more than 0.8 m apart and with 99% accuracy if they are more than 1.1 m apart. This is an improvement of their earlier work [157], where they demonstrated that the observed signal pattern is different when a person is lying on it as opposed to standing on it. They also implement fall detection in a later work [158] by classifying the poses based upon their contact area amongst other metrics.

CapFloor [159] uses two sets of parallel wires orthogonal to each other with each wire forming a capacitive plate in the loading mode. A person walking above alters the measured capacitance in any wire underneath. Since there are two sets of wires in orthogonal directions, a person is above at least one wire in each direction, with the intersection point of these wires being the target's estimated position. Braun *et al.* stated the positioning error to be "in the range of" 0.5 m.

Sensing Floor, presented in [160], employs 36 0.09 m × 0.09 m copper foil squares, spaced 0.01 m apart, embedded underneath 0.6 m × 0.6 m MDF panels. As a foot comes in proximity to the floor, the loading mode capacitance between the floor and the foot is determined by the overlap of the foot and the panel underneath. The measured capacitance forms a low-resolution image that is interpolated to improve the resolution. Subsequent binary thresholding followed by blob detection results in footstep detection. Faulkner *et al*. estimated median position error of 0.0135 m and a median angular error of 10.4° for stationary foot placement. This work is extended [161] to extract various poses for a target lying on the floor and tracking a moving target. The median localization error for a single target moving along a testbed of 2.4 m × 1.2 m over 22 trajectories is 0.022 m.

Akhmareh *et al.* [162] used four loading mode capacitive sensors affixed to the walls. Each sensor, constructed from small copper clad tiles (0.08 m × 0.08 m), is positioned at the center of each wall at a height of 1.15 m from the floor. The tiles are connected to a 555 timer so that the change in capacitance causes a change in output frequency. The system uses fingerprinting to match live samples taken to the nearest grid point. They report 0.2 m mean localization error for static positioning in a 3 m × 3 m room that also had interference sources, such as a fridge and metal cupboard in it. The work is further extended by Tariq *et al.* [163], where they apply multiple ML classifiers and the random forest improves accuracy to 0.05 m. In a later work [164], they improve the sensors to enable mobile target tracking with NN. They report mean error of 0.307 and 0.326 m for 1-D-CNN and long-short term memory (LSTM), respectively.

All the works discussed in this section so far have used loading mode capacitive sensing. TileTrack [165], on the other hand, uses transmit mode sensing. An additional electrode is placed in the room to receive a 32 kHz square wave transmitted from 0.6 m × 0.6 m floor tiles. A target between the electrode and the floor tile changes the amplitude of the square wave. The 80-percentile error for a stationary target is 0.1 m with the largest error of 0.143 m. If a moving target's feet do not fall across multiple tiles, they can only be positioned at the center of that tile. Several different paths are tested with a maximum error of 0.407 m. This work is further extended in [166], where the floor of a 69 m^2 apartment was fitted with either 0.3 m × 0.3 m or 0.6 m × 0.6 m squares. Only the squares close to the target's previous position are tested. If the target "disappears," the whole apartment is searched until they are found again. If the target enters an untracked room, such as the bathroom or the balcony, they are reset to be at the center of that room until they reappear. Tracking is initiated as a person enters (appears) through the front door and is removed if they exit (disappear) by the front door. Some furniture, the sofa and the bed, have contact sensors to further aid with the tracking. They also perform a 14-day living test with an individual living in the apartment as normally as possible. Actions are annotated with a voice recorder so that they can be matched up with the data when it is processed. The 90-percentile localization error is found to be 0.07/0.11 m for standing on 0.3/0.6 m

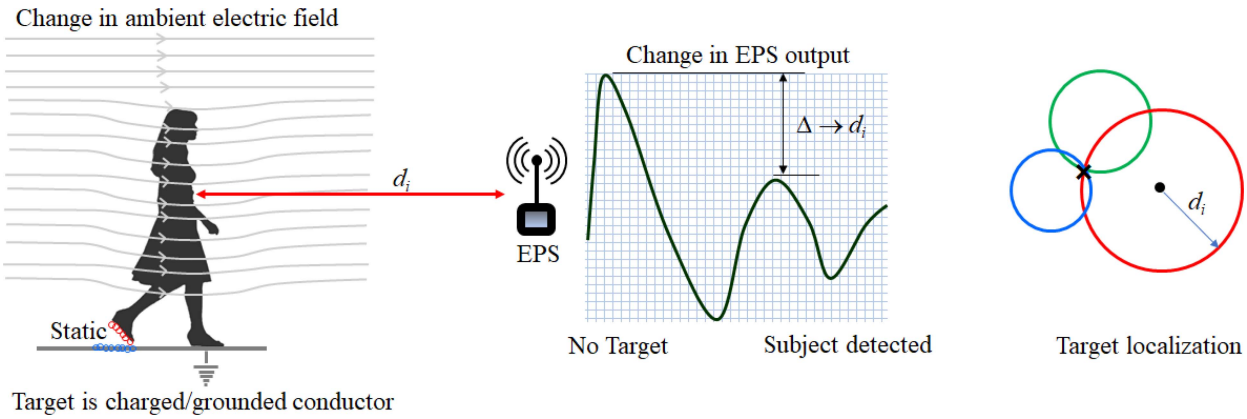

Fig. 9. Passive electric field sensing. The change in ambient electric field is measured by EPS and is used for localization (lateration in this example).

tiles. For moving target, the 90-percentile error is found to be 0.17/0.33 m on 0.3/0.6 m tiles.

B. Localization With Passive Electric Field Sensing

Passive electric field sensing is opportunistic in nature and does not require a transmitted signal. Electric field emitted by the mains (50/60 Hz) powerline and the static electric field between the ground and the ionosphere present themselves as signals of opportunity. These electric fields are perturbed by the movement of an earthed body, i.e., the target [167], and present an opportunity similar to shunt mode active sensing. Also, as a person walks on the floor, static charge and resulting electric potential build up due to the triboelectric effect. The movement of the charged target also causes change in the electric field. Positioning is determined by measuring these changes in the ambient electric field caused by the target. Fig. 9 shows a typical method of localization using passive electric field sensing.

Prance *et al.* [167] measured the change in the AC powerline electric field with the aid of electric potential sensors (EPSs) for target localization. Through experimental data collection, they demonstrate that the electric field's amplitude reduction caused by the target is proportional to the inverse of its distance from the sensor. By measuring the electric field amplitude at four sensors, the ranges of the target are estimated for subsequent localization using lateration. The four sensors are placed along the perimeter of a 3.52 m $\times$ 3.52 m square with each sensor at the midpoint of each side on a 1-m tripod. They quote "localization accuracy" of approximately 0.1 m when the target moves linearly between the opposite pairs of sensors. The accuracy deteriorates for circular and zigzag trajectories. While the estimated trajectories are plotted, no accuracy values are reported for these cases.

Grosse-Puppendahl *et al.* [168] developed Platypus, a combined identification and positioning system. Six EPS are placed on the ceiling at known positions to monitor a 2.5 m $\times$ 2 m area directly underneath. A parametric model is developed to perform ranging based on electric field measurement leading to localization using lateration. The change in electric potential with respect to time is then used to identify said subject. The median position error is found to be 0.13 m for "slow walking" and 0.16 m for "normal walking." User identification is found to be 75% accurate for 30 participants. Fu *et al.* [169] then extend the work by using a grid of passive electrodes constructed from insulated copper wires underneath the floor. Regions of interests are identified based on the activated horizontal and vertical electrodes. The center of the region of interest, which is taken as the footstep's center, is estimated as the weighted average of the activated electrodes' locations. A mean position accuracy of 0.127 m is achieved. While they discuss how the system could potentially perform multitarget tracking, no experimental study for such tracking is reported.

Tang and Mandal [170] derived a parametric model between the reduction in electric field amplitude caused by the target and its distance from the EPS. This calibrated model is used for ranging followed by localization using lateration. They perform localization experiments in an 8 m $\times$ 10 m and a 5 m $\times$ 8 m room with three sensors positioned at 1 m height in each room. The target follows several trajectories and the mean error varies between 0.104 and 0.272 m. Simulations suggest that the localization accuracy can be improved with denser sensor deployment. They are also able to identify between six participants with a 98.3% success rate and attain occupancy estimation ($<$ 10) with an accuracy of 89.03%. They also show that by knowing the number of targets (through occupancy estimation), it is possible to track two targets. With six sensors in a 3 m $\times$ 3.5 m area, they attain mean and 95 percentile errors of 0.2 and 0.78 m, respectively.

Zhou *et al.* [171] developed P-Loc that localizes by measuring the impedance change in the existing electric powerline caused its coupling with the human body. This an extension of E-Loc reported in [172]. In both systems, the impact of the coupling is observed away from the 50/60 Hz AC mains to avoid interference. A 70-MHz sine wave signal is injected into the ground wire and its RSS is measured at multiple sockets along the line to generate the location fingerprint. The impact of noise resulting from ambient changes is mitigated by outlier removal and high pass filtering that assumes that target is faster than the environmental changes. In P-Loc, a multilayer perceptron (MLP) is employed as the classifier to locate the target at a grid level. Further accuracy is achieved through applying a tracking model based on HMM and Viterbi search

algorithm. In contrast, the E-Loc employs an SVM-based classifier for coarse, grid-level localization. Both systems are evaluated in a 6 m × 10 m multiroom test location divided in 1.2 m × 1.2 m grids with five sensors. E-Loc achieves 90.76% localization accuracy in identifying the location within a cell. P-Loc achieves 91.07% grid level accuracy and 0.48 m mean localization error.

Conductive inkjet technology is utilized by Gong *et al.* [173] to exploit both active and passive electric field sensing. Their prototype is essentially a 2.5 m × 0.3 m sensing surface made of flexible substrate that can be deployed on or under the floor. Custom-printed conductive traces on the substrate act as electrodes and antennas for sensing. The sensing tiles are produced by printing a specific copper pattern onto the substrate. Each 0.3 m × 0.3 m sensing tile contains four 0.12 m × 0.12 m printed electrodes. For active sensing, one of the electrodes on each tile transmits a 5-V square wave signal to the other three that are set up as receivers. When the target's body bridges any Tx-Rx pair, the receiver detects a signal whose amplitude is proportional to the capacitive coupling between that electrode pair. Depending on the distance between the target's body and the transmit electrode, the capacitive coupling is either transmit (target very close to the transmitter) or shunt (target not close to the transmitter) mode. While no localization is performed, experiments conducted show that it is possible to correlate the observed signals with footsteps' heel strikes and mid swing. The system is also capable of passive electric field sensing with the electrodes sensing the powerline electric field, which is coupled more strongly when a person stands on them. The change in amplitude depends on the contact area and proximity and therefore can be used to infer the location of the footstep. While no localization experiments are conducted, it is possible to differentiate among heel strikes, forefoot strikes, and mid swings between steps.

Takiguchi *et al.* [174] measured the change in electric field to count the number of steps a subject made with 99.4% accuracy. Kurita [175] then shows that the waveforms produced as an individual walks are unique enough for gait recognition. Kurita is able to identify subjects with a false acceptance rate of 0.61% and a false rejection rate of 2.31%. Many other works have used electric field sensing for applications synergistic with positioning. For an overview of such works, the readers are referred to the survey by Grosse-Puppendahl *et al.* [34].

VI. Conclusion: Challenges and Opportunities

While unobtrusive passive localization using non-RF techniques is an active research field, there are many limitations and unsolved problems leading to exciting research opportunities. In this section, we provide a brief overview of such challenges and opportunities.

A. Sensor Fusion and Utilization of Multiple Technologies

Localization is a multimodal, multisensory, multitechnology problem and therefore, require a multidisciplinary approach. Our survey unfortunately shows a fractured research landscape with "siloed" approach. Among the works presented in this article, LOCI [88] is the only system that utilizes multiple types of sensors. Even this lone example employs a thermopile array in conjunction with a PIR sensor and therefore is limited to only IR sensing. Sensor fusion can make localization systems more robust, eliminate blind spots, add redundancy, and simplify implementation. An ideal IPS should use existing infrastructure of a building and not require the end user to deploy significant additional resources. Rather than installing a large number of bespoke sensors for a single mode solution, it is preferable to utilize preexisting resources, such as Wi-Fi network, PIR motion detectors, structural health monitoring system, etc., and then supplement with other sensors. Utilizing human routine and activities of daily living (ADL) should be considered. The only such example we found is the application of A-star algorithm assisted by an accessibility map (a heatmap constructed from the daily routines of the occupants) by Yang *et al.* [82]. Many localization systems require initialization and estimation of background condition or empty state. Preexisting motion sensors and/or environmental sensors (e.g., CO_2 sensors) can reliably indicate occupancy without having to resort to complex algorithms.

B. Multiple Target Positioning and Tracking

The majority of the reported solutions are able to localize only a single target. This is perfectly acceptable for many applications (e.g., AAL for an elderly individual living alone). Yet, the full potential of DFL can only be unlocked with robust multiple target localization that is often left as a future work by most researchers. Table III lists the articles that have addressed the multitarget problem. Unfortunately, even these solutions have somewhat limited efficacy and only function for a small number of targets (up to a maximum of three among the works validated by experiments). The performance invariably degrades as soon as a second target is introduced. The multitarget solutions are purpose built to work for a set small number of targets, within controlled settings and cannot be generalized for a larger target number. The issue is exacerbated by the fact that unobtrusive passive localization solutions are often opportunistic in nature. There is scope for adopting techniques from other disciplines. However, many inherent challenges, such as complex nature of the medium, dynamically changing environment, significant presence of noise and interference, etc., pose unique difficulties. Therefore, a paradigm shift is required. Multimodal sensing and utilizing knowledge of ADL can be effective. While ML can be a potential solution, they require large training corpus. The time and labor cost of site surveying make data collection a significant challenge. Alternatives, such as crowdsourcing, data fabrication, etc., inherently compromise data quality.

C. Accuracy Evaluation and Reporting

Localization error is commonly used to demonstrate accuracy and precision. But there is no universally adopted error metric. A wide range of accuracy metrics, such as median, mean, percentile, quartiles of localization errors, RMSE, etc., have been used. Active localization discipline has several evaluation guidelines like ISO/IEC 18305 [176] and EvAAL [177], which is used by the indoor positioning and indoor navigation (IPIN) competition. There is also a set of procedures [178]

TABLE III
LIST OF ARTICLES THAT IMPLEMENTED MULTITARGET TRACKING

Research	Sensing Method	No of Targets	Comments
Liau et al. [119], 2008	Pressure (Load Cell)	2	0.2828 m of 85-percentile and 76.25-percentile for 1 and 2 targets.
Hao et al. [65], 2009	Binary PIR	2	Mean error < 0.5 m. No single target performance is quoted.
Rimminen et al. [156], 2009	Active Electric Field	2	Positioning accuracy not specified for 2 targets.[1]
Lauterbach et al. [155], 2012	Active Electric Field	2	Positioning accuracy not specified.
Lan et al. [125], 2017	Binary Pressure	3	Accuracy > 90% for up to 2 targets. ≈ 80% accuracy for 3 targets.[2]
Yang et al. [85], 2019	Binary PIR	2	Mean error < 0.8 m. No single target performance is quoted.
Qu et al. [110], 2019	Thermopile	3	Accuracy not quoted for multi-target.
Shi et al. [142], 2019	Vibration	2	Mean error of 0.65 m. No single target performance is quoted.
Fu et al. [169], 2019	Passive Electric Field	2	Positioning accuracy not specified for 2 target scenario.
Tang & Mandal [170], 2019	Passive Electric Field	2	Mean error 0.104 m - 0.272 m for single and 0.2 m for multi-target.[3]
Yang et al. [87], 2020	Analog PIR	3	Mean errors of 0.43 m, 0.6 m and 0.82 m for 1, 2 and 3 targets.
Narayana et al. [88], 2020	Analog PIR + Thermopile	3	80 percentile errors of 0.35 m and 0.88 m for 1 and 3 targets.[4]

[1]For two target scenario 99% & 90% discrimination performance with gaps of 1.1 m & 0.78 m respectively.
[2]Grid level positioning accuracy on a 3.6 m × 3.6 m testbed divided into a grid of 6 × 6. Needs to know the number of targets.
[3]Single target scenario used 3 sensors. Multi-target scenario used 6 sensors in a much smaller test area.
[4]For multi-target scenario, between 2 and 3 targets were within the FoV of the sensor.

TABLE IV
LIST OF ARTICLES THAT DISCUSS GT RECORDING SYSTEM

Research	Ground Truth System
Rimminen et al. [156], 2009	Customized system; subject wore a hat connected with encoder/pulley.
Prance et al. [167], 2012	Microsoft lifecam VX-3000 USB camera; tracked a yellow dot on the subject's shoulder.
Yin et al. [77], 2016	Bluetooth Tag.
Poston et al. [131], 2017	Custom designed system using PulsedLightmodel LIDAR-Litev2 with precision real-time clock.
Yang et al. [82], 2018	Opti-track Motion Capture system.
Fu et al. [169], 2019	Kinect V2 skeletal tracking.
Faulkner et al. [161], 2020	HTC Vive with two Lighthouses, Tracker affixed to subject's head.
Tariq et al. [164], 2020	Marvelmind robotics ultrasound system; 4 ceiling mounted anchors tracking a tag affixed on a hat worn by the subject.
Yang et al. [87], 2020	UWB-based localization system YCHIOT-MINI3S.

used by the annual Microsoft Indoor Localization Competition. However, these methodologies have not been widely adopted for DFL and may not be even appropriate for evaluating passive positioning systems. A consistent testing procedure is also needed for reporting the performance of positioning systems. Unfortunately, wide variations in the size and other aspects of the test location, density of sensor deployment, etc., make objective evaluation and comparison among various reported systems difficult. All of these issues are compounded when comparing across different technologies and sensing modalities. The accuracy metric should be regularized by the area of coverage, the number of sensors and the cost of implementation. Therefore, it is necessary to develop a universal testing scheme that will allow for an objective, "apple-to-apple" performance comparison.

D. Ground-Truth Accuracy

The localization error is computed as the difference between the position of the target estimated by the system and the actual position of the target or the GT. Therefore, the integrity of the reported accuracy depends on the accuracy of the GT. The GT must be an order of magnitude more accurate than the positioning system. Unfortunately, the majority of the published articles gloss over (e.g., a camera was used to determine the actual position of the target, the target walked along a predefined trajectory) or do not describe this critical step. As can be seen from Table IV, only a handful of the papers provide details about the GT systems utilized. There seems to be an implicit assumption that the GT is accurate. However, published report suggests that GT recording can be significantly inaccurate and a small error in GT measurement can have significant impact on the positioning evaluation [179]. Furthermore, the calibration of parametric models (e.g., distance versus signal attenuation) also requires accurate GT recording. Motion capture technology to capture GT is not economically feasible for most researchers. Options like gaming technology (e.g., Kinect, HTC Vive, etc.) should be investigated for accurate and automated GT recording. An

economically feasible system can also be useful for building ML training corpora.

E. Evaluation in Real-World Environment

The cost of human time and labor limits the collection of data required for calibration, model development, ML training, etc., to a brief period and at a few, sometimes just a single, locations. However, this compromise means that the temporal and spatial variation and diversity are not adequately captured. Similar practical considerations constrain the performance evaluation of the positioning systems. There are several public domain data sets in various ML repositories for wireless DFL. However, the techniques investigated in this article lack such resource, the onus of data collection is on the researchers. Yin *et al.* [77] collected PIR motion sensor data for a year in an apartment with two elderly occupants. But there is no concurrent recording of GT. Even when they collect data over two weeks span with tagged occupants, they use a Bluetooth-based GT recording system that is not very accurate. There are some reported works where mock apartments were used (e.g., [82], [90], [120], and [166]). There are also examples, such as the Smart Condo [71] and INRIA-Nancy smart apartment [122], which were specifically set up for long-term data collection and evaluation. More such efforts are necessary and the lack of opensource data needs to be addressed.

F. Practical Considerations

A localization system has to be readily transferrable from one location to another without significant recalibration. In addition, the indoor environment is also quite dynamic and is inherently unsuited to techniques that require frequent and extensive calibration. A positioning system, which requires significant recalibration whenever a furniture is moved, is not viable for real-world usage. Therefore, there is a need for developing the DFL system that can self-calibrate and adapt to changing scenarios. If necessary, even localization accuracy can be traded off for robustness and less reliance on calibration.

Practical DFL systems need to position and track in real time. In contrast, the majority of the implemented prototypes use data collected during experiments for positioning at a later time. In many cases, the same data are divided into multiple sets with some used for calibration and training and the rest used for performance evaluation. It is difficult to ascertain whether these systems can perform adequately with a different set of sensor data, let alone in real time, at a different location in dynamically changing environment. Also, critical factors, such as computational complexity, energy consumptions, etc., are absent or glossed over in most articles.

Is accuracy the most important consideration while designing a localization system? Benchmarking in terms of accuracy is a staple in the published articles. More consideration needs to be given to practicality, robustness, ease of deployment, and cost. Depending on the application, localization accuracy can be traded off with other performance parameters. As an example, if the goal is to raise alarm in case of a fall, the key accuracy metric should be the detection performance. A "room level" localization accuracy is perfectly acceptable if the system can detect every single fall event without false alarm.

G. Privacy and Security

Location (especially in real-time), daily routine, etc., which are considered to be extremely private information, are collected and stored by an IPS. Therefore, there is an inherent risk of privacy breach. Also, many applications are intended to be used for the elderly who are often more vulnerable to technology centric malicious activities. RF sensing-based localization systems are vulnerable to jamming or spoofing [180], [181]. In passive localization systems, the target does not have a device on their person that can be compromised, or its signal intercepted. Therefore, they are more robust than active localization techniques. The techniques discussed in this article are also inherently more secure than their wireless counterparts. For example, visible light or IR signals are confined within a small area and thus cannot be interfered with without being at close proximity. Floor-based localization systems will require the malicious entity to have physical access to the premises. However, the majority of the techniques discussed in this article utilize/envision the deployment of the sensors as a WSN, potentially within an IoT framework and are therefore vulnerable to an attack to the network just like wireless localization techniques [182]. Marginal processing power and energy constraints make implementing robust security protocols challenging. Security and privacy are well investigated within the IoT discipline [183], [184]. That domain knowledge should be applied in the context of DFL for in situ evaluation and risk analysis, which is currently lacking.

REFERENCES

[1] A. Zanella, N. Bui, A. Castellani, L. Vangelista, and M. Zorzi, "Internet of things for smart cities," *IEEE Internet Things J.*, vol. 1, no. 1, pp. 22–32, Feb. 2014.

[2] J. Z. Liang, N. Corso, E. Turner, and A. Zakhor, "Image based localization in indoor environments," in *Proc. 4th Int. Conf. Comput. Geospatial Res. Appl. (COM. Geo)*, 2013, pp. 70–75.

[3] R. Li, J. Liu, L. Zhang, and Y. Hang, "LIDAR/MEMS IMU integrated navigation (SLAM) method for a small UAV in indoor environments," in *Proc. DGON Inertial Sens. Syst. Symp. (ISS)*, 2014, pp. 1–15.

[4] F. Ijaz, H. K. Yang, A. W. Ahmad, and C. Lee, "Indoor positioning: A review of indoor ultrasonic positioning systems," in *Proc. 15th Int. Conf. Adv. Commun. Technol.*, 2013, pp. 1146–1150.

[5] A. Maddumabandara, H. Leung, and M. Liu, "Experimental evaluation of indoor localization using wireless sensor networks," *IEEE Sensors J.*, vol. 15, no. 9, pp. 5228–5237, Sep. 2015.

[6] H. Xie, T. Gu, X. Tao, H. Ye, and J. Lv, "MaLoc: A practical magnetic fingerprinting approach to indoor localization using smartphones," in *Proc. ACM Int. Joint Conf. Pervasive Ubiquitous Comput.*, 2014, pp. 243–253.

[7] A. Yassin *et al.*, "Recent advances in indoor localization: A survey on theoretical approaches and applications," *IEEE Commun. Surveys Tuts.*, vol. 19, no. 2, pp. 1327–1346, 2nd Quart., 2017.

[8] M. Maheepala, A. Z. Kouzani, and M. A. Joordens, "Light-based indoor positioning systems: A review," *IEEE Sensors J.*, vol. 20, no. 8, pp. 3971–3995, Apr. 2020.

[9] P. Müller, S. Ali-Löytty, J. Lekkala, and R. Piché, "Indoor localisation using aroma fingerprints: A first sniff," in *Proc. 14th Workshop Positioning Navig. Commun.*, 2017, pp. 1–5.

[10] L. M. Candanedo and V. Feldheim, "Accurate occupancy detection of an office room from light, temperature, humidity and CO_2 measurements using statistical learning models," *Energy Build.*, vol. 112, pp. 28–39, Jan. 2016.

[11] M. Gruber, A. Trüschel, and J.-O. Dalenbäck, "CO_2 sensors for occupancy estimations: Potential in building automation applications," *Energy Build.*, vol. 84, pp. 548–556, Dec. 2014.

[12] J. Yang, M. Santamouris, and S. E. Lee, "Review of occupancy sensing systems and occupancy modeling methodologies for the application in institutional buildings," *Energy Build.*, vol. 121, pp. 344–349, Jun. 2016.

[13] P. Remagnino, G. A. Jones, N. Paragios, and C. S. Regazzoni, *Video-Based Surveillance Systems: Computer Vision and Distributed Processing*. Dordrecht, The Netherlands: Kluwer Acad. Publ., 2002.

[14] Y.-L. Hou and G. K. H. Pang, "People counting and human detection in a challenging situation," *IEEE Trans. Syst., Man, Cybern. A, Syst., Humans*, vol. 41, no. 1, pp. 24–33, Jan. 2011.

[15] L. Xia, C.-C. Chen, and J. K. Aggarwal, "Human detection using depth information by kinect," in *Proc. CVPR Workshops*, 2011, pp. 15–22.

[16] M. R. U. Saputra, Q. Chen, Widyawan, G. D. Putra, and P. I. Santosa, "Indoor human tracking application using multiple depth-cameras," in *Proc. Int. Conf. Adv. Comput. Sci. Inf. Syst.*, 2012, pp. 307–312.

[17] M. M. Rapoport, "The home under surveillance: A tripartite assemblage," *Surveillance Soc.*, vol. 10, nos. 3–4, pp. 320–333, 2012.

[18] Y. Ma, G. Zhou, and S. Wang, "WiFi sensing with channel state information: A survey," *ACM Comput. Surveys*, vol. 52, no. 3, pp. 1–36, 2019.

[19] K. Qian, C. Wu, Y. Zhang, G. Zhang, Z. Yang, and Y. Liu, "Widar2.0: Passive human tracking with a single Wi-Fi link," in *Proc. 16th Annu. Int. Conf. Mobile Syst. Appl. Services*, 2018, pp. 350–361.

[20] D. Konings, F. Alam, F. Noble, and E. M.-K. Lai, "Device-free localization systems utilizing wireless RSSI: A comparative practical investigation," *IEEE Sensors J.*, vol. 19, no. 7, pp. 2747–2757, Apr. 2019.

[21] R. C. Shit *et al.*, "Ubiquitous localization (UbiLoc): A survey and taxonomy on device free localization for smart world," *IEEE Commun. Surveys Tuts.*, vol. 21, no. 4, pp. 3532–3564, 4th Quart., 2019.

[22] F. Zafari, A. Gkelias, and K. K. Leung, "A survey of indoor localization systems and technologies," *IEEE Commun. Surveys Tuts.*, vol. 21, no. 3, pp. 2568–2599, 3rd Quart., 2019.

[23] S. Denis, R. Berkvens, and M. Weyn, "A survey on detection, tracking and identification in radio frequency-based device-free localization," *Sensors*, vol. 19, no. 23, p. 5329, 2019.

[24] M. A. Al-qaness *et al.*, "Channel state information from pure communication to sense and track human motion: A survey," *Sensors*, vol. 19, no. 15, p. 3329, 2019.

[25] Z. Yang, C. Wu, Z. Zhou, X. Zhang, X. Wang, and Y. Liu, "Mobility increases localizability: A survey on wireless indoor localization using inertial sensors," *ACM Comput. Surveys*, vol. 47, no. 3, pp. 1–34, 2015.

[26] B. Jang and H. Kim, "Indoor positioning technologies without offline fingerprinting map: A survey," *IEEE Commun. Surveys Tuts.*, vol. 21, no. 1, pp. 508–525, 1st Quart., 2019.

[27] S. He and S.-H. G. Chan, "Wi-Fi fingerprint-based indoor positioning: Recent advances and comparisons," *IEEE Commun. Surveys Tuts.*, vol. 18, no. 1, pp. 466–490, 1st Quart., 2016.

[28] B. Lashkari, J. Rezazadeh, R. Farahbakhsh, and K. Sandrasegaran, "Crowdsourcing and sensing for indoor localization in IoT: A review," *IEEE Sensors J.*, vol. 19, no. 7, pp. 2408–2434, Apr. 2019.

[29] J. Xiao, Z. Zhou, Y. Yi, and L. M. Ni, "A survey on wireless indoor localization from the device perspective," *ACM Comput. Surveys*, vol. 49, no. 2, pp. 1–31, 2016.

[30] J. Luo, L. Fan, and H. Li, "Indoor positioning systems based on visible light communication: State of the art," *IEEE Commun. Surveys Tuts.*, vol. 19, no. 4, pp. 2871–2893, 4th Quart., 2017.

[31] Y. Zhuang *et al.*, "A survey of positioning systems using visible LED lights," *IEEE Commun. Surveys Tuts.*, vol. 20, no. 3, pp. 1963–1988, 3rd Quart., 2018.

[32] M. F. Keskin, A. D. Sezer, and S. Gezici, "Localization via visible light systems," *Proc. IEEE*, vol. 106, no. 6, pp. 1063–1088, Jun. 2018.

[33] M. Afzalan and F. Jazizadeh, "Indoor positioning based on visible light communication: A performance-based survey of real-world prototypes," *ACM Comput. Surveys*, vol. 52, no. 2, pp. 1–36, 2019.

[34] T. Grosse-Puppendahl *et al.*, "Finding common ground: A survey of capacitive sensing in human–computer interaction," in *Proc. CHI Conf. Human Factors Comput. Syst.*, 2017, pp. 3293–3315.

[35] T. Teixeira, G. Dublon, and A. Savvides, "A survey of human-sensing: Methods for detecting presence, count, location, track, and identity," *ACM Comput. Surveys*, vol. 5, no. 1, pp. 59–69, 2010.

[36] R. F. Brena, J. P. García-Vázquez, C. E. Galván-Tejada, D. Muñoz-Rodriguez, C. Vargas-Rosales, and J. Fangmeyer, "Evolution of indoor positioning technologies: A survey," *J. Sensors*, vol. 2017, pp. 1–21, Jan. 2017.

[37] F. Khelifi, A. Bradai, A. Benslimane, P. Rawat, and M. Atri, "A survey of localization systems in Internet of things," *Mobile Netw. Appl.*, vol. 24, no. 3, pp. 761–785, 2019.

[38] H. Yang, W.-D. Zhong, C. Chen, A. Alphones, and P. Du, "QoS-driven optimized design-based integrated visible light communication and positioning for indoor IoT networks," *IEEE Internet Things J.*, vol. 7, no. 1, pp. 269–283, Jan. 2020.

[39] P. H. Pathak, X. Feng, P. Hu, and P. Mohapatra, "Visible light communication, networking, and sensing: A survey, potential and challenges," *IEEE Commun. Surveys Tuts.*, vol. 17, no. 4, pp. 2047–2077, 4th Quart., 2015.

[40] T. Li, C. An, Z. Tian, A. T. Campbell, and X. Zhou, "Human sensing using visible light communication," in *Proc. 21st Annu. Int. Conf. Mobile Comput. Netw.*, Paris, France, 2015, pp. 331–344.

[41] S. Zhang, K. Liu, Y. Ma, X. Huang, X. Gong, and Y. Zhang, "An accurate geometrical multi-target device-free localization method using light sensors," *IEEE Sensors J.*, vol. 18, no. 18, pp. 7619–7632, Sep. 2018, doi: 10.1109/JSEN.2018.2862412.

[42] K. Majeed and S. Hranilovic, "Performance bounds on passive indoor positioning using visible light," *J. Lightw. Technol.*, vol. 38, no. 8, pp. 2190–2200, Apr. 2020.

[43] N. Faulkner, F. Alam, M. Legg, and S. Demidenko, "Watchers on the wall: Passive visible light-based positioning and tracking with embedded light-sensors on the wall," *IEEE Trans. Instrum. Meas.*, vol. 69, no. 5, pp. 2522–2532, May 2020.

[44] T. Li, Q. Liu, and X. Zhou, "Practical human sensing in the light," in *Proc. 14th Annu. Int. Conf. Mobile Syst. Appl. Services*, 2016, pp. 71–84.

[45] D. Konings, N. Faulkner, F. Alam, E. M.-K. Lai, and S. Demidenko, "FieldLight: Device-free indoor human localization using passive visible light positioning and artificial potential fields," *IEEE Sensors J.*, vol. 20, no. 2, pp. 1054–1066, Jan. 2020.

[46] V. Nguyen, M. Ibrahim, S. Rupavatharam, M. Jawahar, M. Gruteser, and R. Howard, "Eyelight: Light-and-shadow-based occupancy estimation and room activity recognition," in *Proc. IEEE Conf. Comput. Commun.*, Apr. 2018, pp. 351–359, doi: 10.1109/INFOCOM.2018.8485867.

[47] E. Di Lascio, A. Varshney, T. Voigt, and C. Pérez-Penichet, "Poster abstract: LocaLight-a battery-free passive localization system using visible light," in *Proc. 15th ACM/IEEE Int. Conf. Inf. Process. Sens. Netw.*, 2016, pp. 1–2.

[48] K. Deprez, S. Bastiaens, L. Martens, W. Joseph, and D. Plets, "Passive visible light detection of humans," *Sensors*, vol. 20, no. 7, p. 1902, 2020.

[49] M. Ibrahim, V. Nguyen, S. Rupavatharam, M. Jawahar, M. Gruteser, and R. Howard, "Visible light based activity sensing using ceiling photosensors," *Proc. 3rd Workshop Visible Light Commun. Syst.*, 2016, pp. 43–48.

[50] K. Majeed and S. Hranilovic, "Passive indoor localization for visible light communication systems," in *Proc. IEEE Global Commun. Conf.*, 2018, pp. 1–6.

[51] A. A. Al-Hameed, S. H. Younus, A. T. Hussein, M. T. Alresheed, and J. M. Elmirghani, "LiDAL: Light detection and localization," *IEEE Access*, vol. 7, pp. 85645–85687, 2019.

[52] A. A. Al-Hameed, S. H. Younus, A. T. Hussein, M. T. Alresheedi, and J. M. Elmirghani, "Artificial neural network for LiDAL systems," *IEEE Access*, vol. 7, pp. 109427–109438, 2019.

[53] Y. Yang, J. Hao, J. Luo, and S. J. Pan, "CeilingSee: Device-free occupancy inference through lighting infrastructure based LED sensing," in *Proc. IEEE Int. Conf. Pervasive Comput. Commun. (PerCom)*, Mar. 2017, pp. 247–256, doi: 10.1109/PERCOM.2017.7917871.

[54] N. Faulkner, F. Alam, M. Legg, and S. Demidenko, "Smart wall: Passive visible light positioning with ambient light only," in *Proc. IEEE Int. Instrum. Meas. Technol. Conf. (I2MTC)*, 2019, pp. 1–6.

[55] D. Konings, B. Parr, F. Alam, and E. M.-K. Lai, "Falcon: Fused application of light based positioning coupled with onboard network localization," *IEEE Access*, vol. 6, pp. 36155–36167, 2018.

[56] D. Konings, F. Alam, F. Noble, and E. M.-K. Lai, "SpringLoc: A device-free localization technique for indoor positioning and tracking using adaptive RSSI spring relaxation," *IEEE Access*, vol. 7, pp. 56960–56973, 2019.

[57] C. Zhang, J. Tabor, J. Zhang, and X. Zhang, "Extending mobile interaction through near-field visible light sensing," in *Proc. 21st Annu. Int. Conf. Mobile Comput. Netw.*, Paris, France, 2015, pp. 345–357.

[58] T. Li, X. Xiong, Y. Xie, G. Hito, X.-D. Yang, and X. Zhou, "Reconstructing hand poses using visible light," *Proc. ACM Interact. Mobile Wearable Ubiquitous Technol.*, vol. 1, no. 3, pp. 1–20, 2017.

[59] R. H. Venkatnarayan and M. Shahzad, "Gesture recognition using ambient light," *Proc. ACM Interact. Mobile Wearable Ubiquitous Technol.*, vol. 2, no. 1, pp. 1–28, 2018.

[60] Q. Hu, Z. Yu, Z. Wang, B. Guo, and C. Chen, "ViHand: Gesture recognition with ambient light," in *Proc. IEEE SmartWorld Ubiquitous Intell. Comput. Adv. Trusted Comput. Scalable Comput. Commun. Cloud Big Data Comput. Internet People Smart City Innovat. (SmartWorld/SCALCOM/UIC/ATC/CBDCom/IOP/SCI)*, 2019, pp. 468–474.

[61] H. Duan, M. Huang, Y. Yang, J. Hao, and L. Chen, "Ambient light based hand gesture recognition enabled by recurrent neural network," *IEEE Access*, vol. 8, pp. 7303–7312, 2020.

[62] C. Lee *et al.*, "Indoor positioning system based on incident angles of infrared emitters," in *Proc. 30th Annu. Conf. IEEE Ind. Electron. Soc.*, 2004, pp. 2218–2222.

[63] B. Song, H. Choi, and H. S. Lee, "Surveillance tracking system using passive infrared motion sensors in wireless sensor network," in *Proc. Int. Conf. Inf. Netw.*, 2008, pp. 1–5.

[64] H. H. Kim, K. N. Ha, S. Lee, and K. C. Lee, "Resident location-recognition algorithm using a Bayesian classifier in the PIR sensor-based indoor location-aware system," *IEEE Trans. Syst., Man, Cybern. C, Appl. Rev.*, vol. 39, no. 2, pp. 240–245, Mar. 2009.

[65] Q. Hao, F. Hu, and Y. Xiao, "Multiple human tracking and identification with wireless distributed pyroelectric sensor systems," *IEEE Syst. J.*, vol. 3, no. 4, pp. 428–439, Dec. 2009.

[66] Q. Hao, F. Hu, and J. Lu, "Distributed multiple human tracking with wireless binary pyroelectric infrared (PIR) sensor networks," in *Proc. IEEE Sens.*, 2010, pp. 946–950.

[67] P. Zappi, E. Farella, and L. Benini, "Tracking motion direction and distance with pyroelectric IR sensors," *IEEE Sensors J.*, vol. 10, no. 9, pp. 1486–1494, Sep. 2010.

[68] G. Monaci and A. Pandharipande, "Indoor user zoning and tracking in passive infrared sensing systems," in *Proc. 20th Eur. Signal Process. Conf. (EUSIPCO)*, 2012, pp. 1089–1093.

[69] C. Jing, B. Zhou, N. Kim, and Y. Kim, "Performance evaluation of an indoor positioning scheme using infrared motion sensors," *Information*, vol. 5, no. 4, pp. 548–557, 2014.

[70] M. Sioutis and Y. Tan, "User indoor location system with passive infrared motion sensors and space subdivision," in *Proc. Int. Conf. Distrib. Ambient Pervasive Interact.*, 2014, pp. 486–497.

[71] I. Vlasenko, I. Nikolaidis, and E. Stroulia, "The Smart-Condo: Optimizing sensor placement for indoor localization," *IEEE Trans. Syst., Man, Cybern., Syst.*, vol. 45, no. 3, pp. 436–453, Mar. 2015.

[72] B. Yang, J. Luo, and Q. Liu, "A novel low-cost and small-size human tracking system with pyroelectric infrared sensor mesh network," *Infrared Phys. Technol.*, vol. 63, pp. 147–156, Mar. 2014.

[73] T. Miyazaki and Y. Kasama, "Multiple human tracking using binary infrared sensors," *Sensors*, vol. 15, no. 6, pp. 13459–13476, 2015.

[74] S. Narayana, R. V. Prasad, V. S. Rao, T. V. Prabhakar, S. S. Kowshik, and M. S. Iyer, "PIR sensors: Characterization and novel localization technique," in *Proc. 14th Int. Conf. Inf. Process. Sensor Netw.*, 2015, pp. 142–153.

[75] B. Yang, Y. Lei, and B. Yan, "Distributed multi-human location algorithm using naive Bayes classifier for a binary pyroelectric infrared sensor tracking system," *IEEE Sensors J.*, vol. 16, no. 1, pp. 216–223, Jan. 2016.

[76] B. Yang, X. Li, and J. Luo, "A novel multi-human location method for distributed binary pyroelectric infrared sensor tracking system: Region partition using PNN and bearing-crossing location," *Infrared Phys. Technol.*, vol. 68, pp. 35–43, Jan. 2015.

[77] J. Yin, M. Fang, G. Mokhtari, and Q. Zhang, "Multi-resident location tracking in smart home through non-wearable unobtrusive sensors," in *Proc. Int. Conf. Smart Homes Health Telematics*, 2016, pp. 3–13.

[78] Y. Li, D. Li, Y. Cheng, G. Liu, J. Niu, and L. Su, "A novel human tracking and localization system based on pyroelectric infrared sensors: Demonstration abstract," in *Proc. 15th Int. Conf. Inf. Process. Sensor Netw.*, 2016, pp. 1–2.

[79] X. Luo, T. Liu, B. Shen, Q. Chen, Widyawan, L. Gao, and X. Luo, "Human indoor localization based on ceiling mounted PIR sensor nodes," in *Proc. 13th IEEE Annu. Consum. Commun. Netw. Conf.*, 2016, pp. 868–874.

[80] X. Luo, Q. Guan, H. Tan, L. Gao, Z. Wang, and X. Luo, "Simultaneous indoor tracking and activity recognition using pyroelectric infrared sensors," *Sensors*, vol. 17, no. 8, p. 1738, 2017.

[81] B. Mukhopadhyay, S. Sarangi, S. Srirangarajan, and S. Kar, "Indoor localization using analog output of pyroelectric infrared sensors," in *Proc. IEEE Wireless Commun. Netw. Conf.*, 2018, pp. 1–6.

[82] D. Yang, B. Xu, K. Rao, and W. Sheng, "Passive infrared (PIR)-based indoor position tracking for smart homes using accessibility maps and a-star algorithm," *Sensors*, vol. 18, no. 2, p. 332, 2018.

[83] L. Wu, Y. Wang, and H. Liu, "Occupancy detection and localization by monitoring nonlinear energy flow of a shuttered passive infrared sensor," *IEEE Sensors J.*, vol. 18, no. 21, pp. 8656–8666, Nov. 2018.

[84] T. Yang, X. Liu, S. Tang, J. Niu, and P. Guo, "Push the limit of PIR sensor based localization," 2019. [Online]. Available: arXiv:1901.10700.

[85] B. Yang, Q. Wei, and L. Yuan, "Location ambiguity resolution and tracking method of human targets in wireless infrared sensor network," *Infrared Phys. Technol.*, vol. 96, pp. 174–183, Jan. 2019.

[86] X. Liu, T. Yang, S. Tang, P. Guo, and J. Niu, "From relative azimuth to absolute location: Pushing the limit of PIR sensor based localization," in *Proc. 26th Annu. Int. Conf. Mobile Comput. Netw.*, 2020, pp. 1–14.

[87] T. Yang, P. Guo, W. Liu, X. Liu, and T. Hao, "A deep-learning-based method for PIR-based multi-person localization," 2020. [Online]. Available: arXiv:2004.04329.

[88] S. Narayana *et al.*, "LOCI: Privacy-aware, device-free, low-power localization of multiple persons using IR sensors," in *Proc. 19th ACM/IEEE Int. Conf. Inf. Process. Sens. Netw.*, 2020, pp. 121–132.

[89] B. Mukhopadhyay, S. Srirangarajan, and S. Kar, "Modeling the analog response of passive infrared sensor," *Sens. Actuators A Phys.*, vol. 279, pp. 65–74, Aug. 2018.

[90] M. P. Fanti, G. Faraut, J.-J. Lesage, and M. Roccotelli, "An integrated framework for binary sensor placement and inhabitants location tracking," *IEEE Trans. Syst., Man, Cybern., Syst.*, vol. 48, no. 1, pp. 154–160, Jan. 2018.

[91] P. Zappi, E. Farella, and L. Benini, "Enhancing the spatial resolution of presence detection in a PIR based wireless surveillance network," in *Proc. IEEE Conf. Adv. Video Signal Based Surveillance*, 2007, pp. 295–300.

[92] L. Wu and Y. Wang, "Shuttered passive infrared sensor for occupancy detection: Exploring a low power electro-mechanical driving approach," in *Proc. ASME Conf. Smart Mater. Adaptive Struct. Intell. Syst.*, 2018.

[93] J. L. Honorato, I. Spiniak, and M. Torres-Torriti, "Human detection using thermopiles," in *Proc. IEEE Lat. Amer. Robot. Symp.*, 2008, pp. 151–157.

[94] J. Kemper and D. Hauschildt, "Passive infrared localization with a probability hypothesis density filter," in *Proc. 7th Workshop Positioning Navig. Commun.*, 2010, pp. 68–76.

[95] M. Kuki, H. Nakajima, N. Tsuchiya, and Y. Hata, "Human movement trajectory recording for home alone by thermopile array sensor," in *Proc. IEEE Int. Conf. Syst. Man Cybern. (SMC)*, 2012, pp. 2042–2047.

[96] H. M. Ng, "Poster abstract: Human localization and activity detection using thermopile sensors," in *Proc. ACM/IEEE Int. Conf. Inf. Process. Sens. Netw. (IPSN)*, 2013, pp. 337–338.

[97] P. Hevesi, S. Wille, G. Pirkl, N. Wehn, and P. Lukowicz, "Monitoring household activities and user location with a cheap, unobtrusive thermal sensor array," in *Proc. ACM Int. Joint Conf. Pervasive Ubiquitous Comput.*, 2014, pp. 141–145.

[98] C. Basu and A. Rowe, "Tracking motion and proxemics using thermal-sensor array," 2015. [Online]. Available: arXiv:1511.08166.

[99] W.-H. Chen and H.-P. Ma, "A fall detection system based on infrared array sensors with tracking capability for the elderly at home," in *Proc. 17th Int. Conf. E-Health Netw. Appl. Services (HealthCom)*, 2015, pp. 428–434.

[100] Z. Chen, Y. Wang, and H. Liu, "Unobtrusive sensor-based occupancy facing direction detection and tracking using advanced machine learning algorithms," *IEEE Sensors J.*, vol. 18, no. 15, pp. 6360–6368, Aug. 2018.

[101] C. Kowalski, K. Blohm, S. Weiss, M. Pfingsthorn, P. Gliesche, and A. Hein, "Multi low-resolution infrared sensor setup for privacy-preserving unobtrusive indoor localization," in *Proc. ICT4AWE*, 2019, pp. 183–188.

[102] A. A. Trofimova, A. Masciadri, F. Veronese, and F. Salice, "Indoor human detection based on thermal array sensor data and adaptive background estimation," *J. Comput. Commun.*, vol. 5, no. 4, pp. 16–28, 2017.

[103] A. Hayashida, V. Moshnyaga, and K. Hashimoto, "The use of thermal IR array sensor for indoor fall detection," in *Proc. IEEE Int. Conf. Syst. Man Cybern. (SMC)*, 2017, pp. 594–599.

[104] Y. Karayaneva, S. Baker, B. Tan, and Y. Jing, "Use of low-resolution infrared pixel array for passive human motion movement and recognition," in *Proc. 32nd Int. BCS Human Comput. Interact. Conf.*, 2018, pp. 1–2.

[105] I. Lorato, T. Bakkes, S. Stuijk, M. Meftah, and G. De Haan, "Unobtrusive respiratory flow monitoring using a thermopile array: A feasibility study," *Appl. Sci.*, vol. 9, no. 12, p. 2449, 2019.

[106] M. Gochoo *et al.*, "Novel IoT-based privacy-preserving yoga posture recognition system using low-resolution infrared sensors and deep learning," *IEEE Internet Things J.*, vol. 6, no. 4, pp. 7192–7200, Aug. 2019.

[107] M. Kuki, H. Nakajima, N. Tsuchiya, K. Kuramoto, S. Kobashi, and Y. Hata, "Mining multi human locations using thermopile array sensors," in *Proc. IEEE 43rd Int. Symp. Multiple Valued Logic*, 2013, pp. 59–64.

[108] M. Kuki, H. Nakajima, N. Tsuchiya, and Y. Hata, "Multi-human locating in real environment by thermal sensor," in *Proc. IEEE Int. Conf. Syst. Man Cybern.*, 2013, pp. 4623–4628.

[109] A. D. Shetty, Disha, B. Shubha, and K. Suryanarayana, "Detection and tracking of a human using the infrared thermopile array sensor—'Grid-EYE,"' in *Proc. Int. Conf. Intell. Comput. Instrum. Control Technol. (ICICICT)*, 2017, pp. 1490–1495.

[110] D. Qu, B. Yang, and N. Gu, "Indoor multiple human targets localization and tracking using thermopile sensor," *Infrared Phys. Technol.*, vol. 97, pp. 349–359, Mar. 2019.

[111] H. Santo, T. Maekawa, and Y. Matsushita, "Device-free and privacy preserving indoor positioning using infrared retro-reflection imaging," in *Proc. IEEE Int. Conf. Pervasive Comput. Commun. (PerCom)*, 2017, pp. 141–152.

[112] A. Pedotti, "Simple equipment used in clinical practice for evaluation of locomotion," *IEEE Trans. Biomed. Eng.*, vol. BME-24, no. 5, pp. 456–461, Sep. 1977.

[113] M. D. Addlesee, A. Jones, F. Livesey, and F. Samaria, "The ORL active floor [sensor system]," *IEEE Pers. Commun.*, vol. 4, no. 5, pp. 35–41, Oct. 1997.

[114] R. J. Orr and G. D. Abowd, "The smart floor: A mechanism for natural user identification and tracking," in *Proc. Extended Abstracts Human Factors Comput. Syst.*, 2000, pp. 275–276.

[115] Y. Kaddoura, J. King, and A. Helal, "Cost-precision tradeoffs in unencumbered floor-based indoor location tracking," in *Proc. 3rd Int. Conf. Smart Homes Health Telematic (ICOST)*, 2005.

[116] J. Paradiso, C. Abler, K.-Y. Hsiao, and M. Reynolds, "The magic carpet: Physical sensing for immersive environments," in *Proc. Extended Abstracts Human Factors Comput. Syst.*, 1997, pp. 277–278.

[117] S. Pirttikangas, J. Suutala, J. Riekki, and J. Röning, "Learning vector quantization in footstep identification," in *Proc. 3rd IASTED Int. Conf. Artif. Intell. Appl.*, 2003, pp. 413–417.

[118] L. McElligott, M. Dillon, K. Leydon, B. Richardson, M. Fernström, and J. A. Paradiso, "'ForSe FIElds'-force sensors for interactive environments," in *Proc. Int. Conf. Ubiquitous Comput.*, 2002, pp. 168–175.

[119] W.-H. Liau, C.-L. Wu, and L.-C. Fu, "Inhabitants tracking system in a cluttered home environment via floor load sensors," *IEEE Trans. Autom. Sci. Eng.*, vol. 5, no. 1, pp. 10–20, Jan. 2008.

[120] M. Andries, O. Simonin, and F. Charpillet, "Localization of humans, objects, and robots interacting on load-sensing floors," *IEEE Sensors J.*, vol. 16, no. 4, pp. 1026–1037, Feb. 2016.

[121] N. Pépin, O. Simonin, and F. Charpillet, "Intelligent tiles-putting situated multi-agents models in real world," in *Proc. ICAART*, 2009, pp. 513–519.

[122] M. Daher, A. Diab, M. E. B. El Najjar, M. A. Khalil, and F. Charpillet, "Elder tracking and fall detection system using smart tiles," *IEEE Sensors J.*, vol. 17, no. 2, pp. 469–479, Jan. 2017.

[123] I. Al-Naimi and C. B. Wong, "Indoor human detection and tracking using advanced smart floor," in *Proc. 8th Int. Conf. Inf. Commun. Syst. (ICICS)*, 2017, pp. 34–39.

[124] T. Murakita, T. Ikeda, and H. Ishiguro, "Human tracking using floor sensors based on the Markov chain Monte Carlo method," in *Proc. 17th Int. Conf. Pattern Recognit.*, 2004, pp. 917–920.

[125] G. Lan, J. Liang, G. Liu, and Q. Hao, "Development of a smart floor for target localization with Bayesian binary sensing," in *Proc. IEEE 31st Int. Conf. Adv. Inf. Netw. Appl. (AINA)*, 2017, pp. 447–453.

[126] G. Lan, X. Hu, and Q. Hao, "A Bayesian approach for targets localization using binary sensor networks," in *Proc. 8th Int. Symp. Comput. Intell. Design (ISCID)*, 2015, pp. 453–456.

[127] T. K. Agrawal, S. Thomassey, C. Cochrane, G. Lemort, and V. Koncar, "Low-cost intelligent carpet system for footstep detection," *IEEE Sensors J.*, vol. 17, no. 13, pp. 4239–4247, Jul. 2017.

[128] J. Yun, S.-H. Lee, W.-T. Woo, and J.-H. Ryu, "The user identification system using walking pattern over the ubifloor," in *Proc. Int. Conf. Control Autom. Syst.*, 2003, pp. 1046–1050.

[129] L. Middleton, A. A. Buss, A. Bazin, and M. S. Nixon, "A floor sensor system for gait recognition," in *Proc. IEEE Workshop Autom. Identification Adv. Technol. (AutoID)*, 2005, pp. 171–176.

[130] J. A. Cantoral-Ceballos *et al.*, "Intelligent carpet system, based on photonic guided-path tomography, for gait and balance monitoring in home environments," *IEEE Sensors J.*, vol. 15, no. 1, pp. 279–289, Jan. 2015.

[131] J. D. Poston, R. M. Buehrer, and P. A. Tarazaga, "Indoor footstep localization from structural dynamics instrumentation," *Mech. Syst. Signal Process.*, vol. 88, pp. 224–239, May 2017.

[132] C. A. Tokognon, B. Gao, G. Y. Tian, and Y. Yan, "Structural health monitoring framework based on Internet of Things: A survey," *IEEE Internet Things J.*, vol. 4, no. 3, pp. 619–635, Jun. 2017.

[133] W. Chen, M. Guan, L. Wang, R. Ruby, and K. Wu, "FLoc: Device-free passive indoor localization in complex environments," in *Proc. IEEE Int. Conf. Commun. (ICC)*, 2017, pp. 1–6.

[134] R. Bahroun, O. Michel, F. Frassati, M. Carmona, and J.-L. Lacoume, "New algorithm for footstep localization using seismic sensors in an indoor environment," *J. Sound Vib.*, vol. 333, no. 3, pp. 1046–1066, 2014.

[135] M. Mirshekari, S. Pan, J. Fagert, E. M. Schooler, P. Zhang, and H. Y. Noh, "Occupant localization using footstep-induced structural vibration," *Mech. Syst. Signal Process.*, vol. 112, pp. 77–97, Nov. 2018.

[136] M. Mirshekari, J. Fagert, S. Pan, P. Zhang, and H. Y. Noh, "Step-level occupant detection across different structures through footstep-induced floor vibration using model transfer," *J. Eng. Mech.*, vol. 146, no. 3, 2020, Art. no. 04019137.

[137] M. Mirshekari, S. Pan, P. Zhang, and H. Y. Noh, "Characterizing wave propagation to improve indoor step-level person localization using floor vibration," in *Proc. Sens. Smart Struct. Technol. Civil Mech. Aerosp. Syst.*, 2016, Art. no. 980305.

[138] S. Pan, A. Bonde, J. Jing, L. Zhang, P. Zhang, and H. Y. Noh, "BOES: Building occupancy estimation system using sparse ambient vibration monitoring," in *Proc. Sens. Smart Struct. Technol. Civil Mech. Aerosp. Syst.*, 2014, Art. no. 90611O.

[139] J. Clemente, F. Li, M. Valero, and W. Song, "Smart seismic sensing for indoor fall detection, location, and notification," *IEEE J. Biomed. Health Inform.*, vol. 24, no. 2, pp. 524–532, Feb. 2019.

[140] S. Pan *et al.*, "Footprintid: Indoor pedestrian identification through ambient structural vibration sensing," *Proc. ACM Interact. Mobile Wearable Ubiquitous Technol.*, vol. 1, no. 3, pp. 1–31, 2017.

[141] S. Pan, M. Mirshekari, P. Zhang, and H. Y. Noh, "Occupant traffic estimation through structural vibration sensing," in *Proc. Sens. Smart Struct. Technol. Civil Mech. Aerosp. Syst.*, 2016, Art. no. 980306.

[142] L. Shi *et al.*, "Device-free multiple people localization through floor vibration," in *Proc. 1st ACM Int. Workshop Device Free Human Sens.*, 2019, pp. 57–61.

[143] J. D. Poston, R. M. Buehrer, A. G. Woolard, and P. A. Tarazaga, "Indoor positioning from vibration localization in smart buildings," in *Proc. IEEE/ION Position Location Navig. Symp. (PLANS)*, 2016, pp. 366–372.

[144] J. D. Poston, "Toward tracking multiple building occupants by footstep vibrations," in *Proc. IEEE Global Conf. Signal Inf. Process. (GlobalSIP)*, 2018, pp. 86–90.

[145] S. E. Alajlouni and P. Tarazaga, "A new fast and calibration-free method for footstep impact localization in an instrumented floor," *J. Vibration Control*, vol. 25, no. 10, pp. 1629–1638, 2019.

[146] P. A. Tarazaga, "Evaluation of a new energy-based human tracking method in a smart building using floor vibration measurements," in *Dynamics of Civil Structures*, vol. 2. Cham, Switzerland: Springer, 2019, pp. 289–292.

[147] S. Drira, Y. Reuland, N. F. Olsen, S. G. Pai, and I. F. C. Smith, "Occupant-detection strategy using footstep-induced floor vibrations," in *Proc. 1st ACM Int. Workshop Device Free Human Sens.*, 2019, pp. 31–34.

[148] M. Lam, M. Mirshekari, S. Pan, P. Zhang, and H. Y. Noh, "Robust occupant detection through step-induced floor vibration by incorporating structural characteristics," in *Dynamics of Coupled Structures*, vol. 4. Cham, Switzerland: Springer, 2016, pp. 357–367.

[149] S. Drira, Y. Reuland, and I. F. C. Smith, "Model-based interpretation of floor vibrations for indoor occupant tracking," in *Proc. 26th Int. Workshop Intell. Comput. Eng.*, 2019.

[150] T. G. Zimmerman, J. R. Smith, J. A. Paradiso, D. Allport, and N. Gershenfeld, "Applying electric field sensing to human–computer interfaces," in *Proc. SIGCHI Conf. Human Factors Comput. Syst.*, 1995, pp. 280–287.
[151] J. Smith, T. White, C. Dodge, J. Paradiso, N. Gershenfeld, and D. Allport, "Electric field sensing for graphical interfaces," *IEEE Comput. Graph. Appl.*, vol. 18, no. 3, pp. 54–60, May/Jun. 1998.
[152] D. Savio and T. Ludwig, "Smart carpet: A footstep tracking interface," in *Proc. 21st Int. Conf. Adv. Inf. Netw. Appl. Workshops*, 2007, pp. 754–760.
[153] C. Lauterbach, A. Steinhage, and A. Techmer, "Large-area wireless sensor system based on smart textiles," in *Int. Multi Conf. Syst. Signals Devices*, 2012, pp. 1–2.
[154] C. Lauterbach, A. Steinhage, and A. Techmer, "A large-area sensor system underneath the floor for ambient assisted living applications," in *Pervasive Mobile Sensing and Computing for Healthcare*. Heidelberg, Germany: Springer, 2013, pp. 69–87.
[155] M. Sousa, A. Techmer, A. Steinhage, C. Lauterbach, and P. Lukowicz, "Human tracking and identification using a sensitive floor and wearable accelerometers," in *IEEE Int. Conf. Pervasive Comput. Commun. (PerCom)*, 2013, pp. 166–171.
[156] H. Rimminen, J. Lindström, and R. Sepponen, "Positioning accuracy and multi-target separation with a human tracking system using near field imaging," *Int. J. Smart Sens. Intell. Syst.*, vol. 2, no. 1, pp. 156–175, 2009.
[157] R. Henry, L. Matti, and S. Raimo, "Human tracking using near field imaging," in *Proc. 2nd Int. Conf. Pervasive Comput. Technol. Healthcare*, 2008, pp. 148–151.
[158] H. Rimminen, J. Lindström, M. Linnavuo, and R. Sepponen, "Detection of falls among the elderly by a floor sensor using the electric near field," *IEEE Trans. Inf. Technol. Biomed.*, vol. 14, no. 6, pp. 1475–1476, Nov. 2010.
[159] A. Braun, H. Heggen, and R. Wichert, "CapFloor–A flexible capacitive indoor localization system," in *Proc. Int. Competition Eval. AAL Syst. Through Competitive Benchmarking*, 2011, pp. 26–35.
[160] N. Faulkner, B. Parr, F. Alam, M. Legg, and S. Demidenko, "Device free localization with capacitive sensing floor," in *Proc. IEEE Sens. Appl. Symp. (SAS)*, Mar. 2020, pp. 1–5.
[161] N. Faulkner, B. Parr, F. Alam, M. Legg, and S. Demidenko, "CapLoc: Capacitive sensing floor for device-free localization and fall detection," *IEEE Access*, vol. 8, pp. 187353–187364, 2020.
[162] A. R. Akhmareh, M. T. Lazarescu, O. Bin Tariq, and L. Lavagno, "A tagless indoor localization system based on capacitive sensing technology," *Sensors*, vol. 16, no. 9, p. 1448, 2016.
[163] O. B. Tariq, M. T. Lazarescu, J. Iqbal, and L. Lavagno, "Performance of machine learning classifiers for indoor person localization with capacitive sensors," *IEEE Access*, vol. 5, pp. 12913–12926, 2017.
[164] O. B. Tariq, M. T. Lazarescu, and L. Lavagno, "Neural networks for indoor human activity reconstructions," *IEEE Sensors J.*, vol. 20, no. 22, pp. 13571–13584, Nov. 2020.
[165] M. Valtonen, J. Maentausta, and J. Vanhala, "Tiletrack: Capacitive human tracking using floor tiles," in *Proc. IEEE Int. Conf. Pervasive Comput. Commun.*, 2009, pp. 1–10.
[166] M. Valtonen, T. Vuorela, L. Kaila, and J. Vanhala, "Capacitive indoor positioning and contact sensing for activity recognition in smart homes," *J. Ambient Intell. Smart Environ.*, vol. 4, no. 4, pp. 305–334, 2012.
[167] H. Prance, P. Watson, R. J. Prance, and S. T. Beardsmore-Rust, "Position and movement sensing at metre standoff distances using ambient electric field," *Meas. Sci. Technol.*, vol. 23, no. 11, 2012, Art. no. 115101.
[168] T. Grosse-Puppendahl *et al.*, "Platypus: Indoor localization and identification through sensing of electric potential changes in human bodies," in *Proc. 14th Annu. Int. Conf. Mobile Syst. Appl. Services*, 2016, pp. 17–30.
[169] B. Fu, F. Kirchbuchner, J. von Wilmsdorff, T. Grosse-Puppendahl, A. Braun, and A. Kuijper, "Performing indoor localization with electric potential sensing," *J. Ambient Intell. Humanized Comput.*, vol. 10, no. 2, pp. 731–746, 2019.
[170] X. Tang and S. Mandal, "Indoor occupancy awareness and localization using passive electric field sensing," *IEEE Trans. Instrum. Meas.*, vol. 68, no. 11, pp. 4535–4549, Nov. 2019.
[171] T. Zhou *et al.*, "P-Loc: A device-free indoor localization system utilizing building power-line network," in *Proc. ACM Int. Joint Conf. Pervasive Ubiquitous Comput. Proc. ACM Int. Symp. Wearable Comput.*, 2019, pp. 611–615.
[172] T. Zhou, Y. Zhang, X. Chen, P. Zhang, and L. Zhang, "E-Loc: Indoor localization through building electric wiring: Poster abstract," in *Proc. 16th ACM/IEEE Int. Conf. Inf. Process. Sensor Netw.*, 2017, pp. 311–312.
[173] N.-W. Gong, S. Hodges, and J. A. Paradiso, "Leveraging conductive Inkjet technology to build a scalable and versatile surface for ubiquitous sensing," in *Proc. 13th Int. Conf. Ubiquitous Comput.*, 2011, pp. 45–54.
[174] K. Takiguchi, T. Wada, and S. Toyama, "Human body detection that uses electric field by walking," *J. Adv. Mech. Design Syst. Manuf.*, vol. 1, no. 3, pp. 294–305, 2007.
[175] K. Kurita, "Human identification from walking signal based on measurement of current generated by electrostatic induction," *Kansei Eng. Int. J.*, vol. 11, no. 4, pp. 183–189, 2012.
[176] *Information Technology—Real Time Locating Systems—Test and Evaluation of Localization and Tracking Systems*, ISO/IEC Standard 18305:2016, Jan. 2016.
[177] F. Potortì *et al.*, "Comparing the performance of indoor localization systems through the EvAAL framework," *Sensors*, vol. 17, no. 10, p. 2327, 2017.
[178] D. Lymberopoulos and J. Liu, "The microsoft indoor localization competition: Experiences and lessons learned," *IEEE Signal Process. Mag.*, vol. 34, no. 5, pp. 125–140, Sep. 2017.
[179] A. Popleteev, "HIPS: Human-based indoor positioning system," in *Proc. Int. Conf. Indoor Positioning Indoor Navig. (IPIN)*, 2016, pp. 1–7.
[180] S. Kim, S. Ha, A. Saad, and J. Kim, "Indoor positioning system techniques and security," in *Proc. 4th Int. Conf. E-Technol. Netw. Develop. (ICeND)*, 2015, pp. 1–4.
[181] J. Cho, J. Yu, S. Oh, J. Ryoo, J. Song, and H. Kim, "Wrong siren! A location spoofing attack on indoor positioning systems: The starbucks case study," *IEEE Commun. Mag.*, vol. 55, no. 3, pp. 132–137, Mar. 2017.
[182] S. Tiku and S. Pasricha, "Overcoming security vulnerabilities in deep learning-based indoor localization frameworks on mobile devices," *ACM Trans. Embedded Comput. Syst. (TECS)*, vol. 18, no. 6, pp. 1–24, 2019.
[183] Y. Yang, L. Wu, G. Yin, L. Li, and H. Zhao, "A survey on security and privacy issues in Internet-of-Things," *IEEE Internet Things J.*, vol. 4, no. 5, pp. 1250–1258, Oct. 2017.
[184] M. Frustaci, P. Pace, G. Aloi, and G. Fortino, "Evaluating critical security issues of the IoT world: Present and future challenges," *IEEE Internet Things J.*, vol. 5, no. 4, pp. 2483–2495, Aug. 2018.

Fakhrul Alam (Senior Member, IEEE) received the B.Sc. degree (Hons.) in electrical and electronic engineering from BUET, Dhaka, Bangladesh, in 1996, and the M.S. and Ph.D. degrees in electrical engineering from Virginia Tech, Blacksburg, VA, USA, in 1999 and 2002, respectively.

He is an Associate Professor with the Department of Mechanical and Electrical Engineering, School of Food and Advanced Technology, Massey University, Auckland, New Zealand. His research interests include indoor localization, 5G and visible light communication, and IoT and wireless sensor networks.

Nathaniel Faulkner received the B.E. degree (Hons.) in electronic and computer engineering from Massey University, Auckland, New Zealand, in 2016, where he is currently pursuing the Ph.D. degree.

His research interests include indoor positioning, embedded systems design, and Internet of Things.

Baden Parr received the B.E. degree (Hons.) in electronics and computer engineering from Massey University, Auckland, New Zealand, in 2017, where he is currently pursuing the Ph.D. degree.

His research interests include 3-D camera technology, indoor localization, acoustic imaging, IoT sensor networks, and robot design.